DATA-DRIVEN UNCERTAINTY IN SEBS BASED ESTIMATES OF EVAPOTRANSPIRATION

ALBERT ANNING AGYAPONG

April, 2013

SUPERVISORS:
Dr. N.A.S. Hamm
Dr. Z. Vekerdy

DATA-DRIVEN UNCERTAINTY IN SEBS BASED ESTIMATES OF EVAPOTRANSPIRATION

ALBERT ANNING AGYAPONG
Enschede, The Netherlands, [April, 2013]

Thesis submitted to the Faculty of Geo-Information Science and Earth Observation of the University of Twente in partial fulfilment of the requirements for the degree of Master of Science in Geo-information Science and Earth Observation.
Specialization: Geoinformatics

SUPERVISORS:
Dr. N.A.S. Hamm
Dr. Z. Vekerdy

THESIS ASSESSMENT BOARD:
Prof.Dr.Ir. A. Stein (Chair)
[Dr.Ir. M.J. Booij (External Examiner, University of Twente)]

ABSTRACT

Evapotranspiration (ET) is a vital component of the water budget and it accurate estimation. Surface Energy Balance System (SEBS) is a model that uses remotely sensed data in combination with meteorological data to estimate evapotranspiration. SEBS in the estimation of ET uses albedo, emissivity, land surface temperature, vegetation index; leaf area index and land cover type from MODIS. For this study, in situ meteorological data used include temperature, wind speed, sunshine hours coupled with other meteorological from the ECMWF products. Sources of uncertainty in any of the mentioned input data will have considerable effect on the output thereby hampering the ability to give informed decisions.

Sources of uncertainty in the in situ meteorological data are the main focus of the study in the Black Volta Basin of Ghana. MATLAB was used in the estimation of ET from SEBS. The Monte Carlo simulation method was used in the analysis of uncertainty in the input data and how it affects the output ET. Monte Carlo method uses a set of probability distribution function generated from the input sources of uncertainty. The results provided evidence of uncertainty in the output data giving a range of input uncertainty from temperature, wind speed and sunshine hours.

SEBS provided baseline actual ET estimates in the rate of 2.88mm to 6.44mm daily and the Monte Carlo simulation of SEBS gave a mean daily actual ET rate of 2.99mm to 6.44mm. Standard deviation ranges from 0.03mm to 1.38mm across stations. Actual ET estimates based on SEBS is affected by uncertainty in input in situ meteorological data.

Keywords: Evapotranspiration, SEBS, MODIS, ECMWF, remote sensing, uncertainty, Black Volta Basin

ACKNOWLEDGEMENT

First of all I would to express my utmost gratitude to the Almighty God for making it possible for me to achieve the aim of an MSc and for His protection and guidance throughout my stay in Netherlands and ITC-University of Twente as a whole.

I thank the Netherlands fellowship programme (NFP) for the initial opportunity to pursue further studies in ITC-University of Twente. My most profound gratitude goes to the TIGER capacity building facility for offering me the opportunity to make my further studies an MSc when all hope seemed to have been lost.

My sincere appreciation goes to my first supervisor Dr. Nicholas Hamm for his immense support and guidance. To Dr. Zoltan Vekerdy, I say a big thank you firstly for your help in securing funds through the TIGER capacity building facility for the continuation of my MSc and secondly for your great support throughout my thesis period as the second supervisor. I would like to express my appreciation to Dr. J. (Joris) Timmermans for providing the MATLAB code that was used to estimate actual evapotranspiration through SEBS. I also appreciate all help and support in further developments to SEBS for the thesis. Further appreciation goes to Gabriel Parodi for his support and guidance in the understanding of SEBS. I am also very grateful to Vincent Omondi Odongo and Rahul Raj for their advice and support.

Special thanks go to Dr. Kwabena Kankam Yeboah of CSIR-Water Research Institute (WRI) for his advice, encouragement and support throughout this period. I would also like to acknowledge Mr Andrew Yaw Nkansah of Ghana Meteorological Agency (GMA) for his enormous help in securing data used for this thesis.

I would like to thank my course director Dr. Connie Blok and the entire administrative staff of GFM for all the support offered me through my stay.

To my family, I say a big thank for your support, prayers and encouragement. Especially Nana Asamoah Boadu and Mama Lucy, may God bless you abundantly. My mum Comfort Ofosu Afriyie, Christopher, Keon and my sweet heart Maame Pomaah Anning Agyapong. My love to you all, God bless you.

Albert Anning Agyapong
Enschede, The Netherlands.
April 2013.

TABLE OF CONTENTS

LIST OF FIGURES

LIST OF TABLES

LIST OF ACRONYMNS

AATSR	Advanced Along-Track Scanning Radiometer
BIPM	Bureau International des Poids et Mesures
ECMWF	European Centre for Medium-Range Weather Forecasts
ECS	EOSDIS Core System
EPS	Ensemble Prediction System
ET	Evapotranspiration
ETa	Actual Evapotranspiration
FAO	Food and Agriculture Organisation
GUM	Guide to the expression of uncertainty in measurement
HDF	Hierarchical Data Format
IEC	International Electro-technical Commission
IFCC	International Federation of Clinical Chemistry
ISO	International Organization for Standardization
IUPAC	International Union of Pure and Applied Chemistry
IUPAP	International Union of Pure and Applied Physics
JCGM	Joint Committee for Guides in Metrology
LP DAAC	Land Processes Distributed Active Archive Centre
LWR	Long Wave Radiation
MODIS	Moderate Resolution Imaging Spectroradiometer
NDVI	Normalized Difference Vegetation Index
NIR	Near Infrared Spectrum
OlML	International Organization of Legal Metrology
PDF	Probability Distribution Function
PV	iso-potential Vorticity
RMSE	Root Mean Square Error
SWR	Short Wave Radiation
SEBS	Surface Energy Balance Systems
SD	Standard Deviation
TIR	Thermal Infrared Spectrum
VIS	Visible Infrared Spectrum
WMO	World Meteorological Organisation

1. INTRODUCTION

1.1. Background

Evapotranspiration (ET) is an important component of the water budget. Understanding its spatial dynamics is of vital importance for food security and water resource management. It accounts for a substantial amount of the water flux in both semi-arid and arid regions across the globe. ET plays a crucial role in the understanding of the terrestrial climate system. It forms part of the surface energy balance system and its effects in the water balance of a particular catchment area is well noticed. Researchers and decision makers use ET to make informed decisions on land use.

In the last half-century, there has been an increase in the variability of the hydrological scheme of the Volta basin located in West Africa. Recent studies have reported some important land surface changes in the area, e.g. the well-known HAPEX Sahel studies (Prince et al., 1995); climate variability studies by (Paturel et al., 1997), rainfall-runoff variability studies by (Gyau-Boakye & Tumbulto, 2000)and vegetation effects on soil wetness by (Opoku-Duah et al., 1999). An important reason underlying the increased atmospheric and surface variability is the complex interrelationships between anthropogenic impacts on the area (e.g. increasing population translating into competition in land use) and climate change impacts (e.g. Sahel region). These studies partly show that rainfall over several areas of the basin has declined considerably since 1970. As a result, stream flows of some catchments, e.g. Saboba and Nawuni (Ghana) have reduced by 32.5% and 23.1%, respectively (Gyau-Boakye & Tumbulto, 2000). Paturel et al. (1997) have also demonstrated that land surface deterioration (i.e. soil and vegetation deterioration) has significantly contributed to approximately, 1% rise in temperature from 1945 till 1993. This has consequently increased the affinity of surrounding air for atmospheric water vapour by approximately 5-6%, thus, increasing regional evapotranspiration losses (Gyau-Boakye & Tumbulto, 2000). The overall effect is the decline of lake levels at the Akosombo dam site (downstream) leading to massive hydro-electric power rationing for most of the year.

Evapotranspiration calculation has always been based on field measurements in the most general cases. Its validity is limited to the local catchment areas (Elhag et al., 2011). Variables used in the estimation of ET are measured from a weather station. Measurements from these variables only provide estimates that are specific to the location in question with no emphasis on the spatial variability of the weather station. Nevertheless, accurate estimation of ET helps in management practices at both local and regional scales. Introducing technology such as Earth observation and remote sensing to compliment on-going activities in the modelling of hydrology and hydro-geology is an important step. Penman Montieth, eddy covariance and many more have been used to carry out ET measurement in lot of research papers including Cai et al. (2007) and Allen (2000). Allen et al. (2011) concluded that accuracy of ET measurements largely varies. Allen et al. (2011) also explained that there are uncertainties as a result of variations in instrument calibration, measurement errors, inadequate measuring instruments or the variability that come with location of weather stations

Taking the Volta basin into account (see Figure 2:1), Gyau-Boakye and Tumbulto (2000) and Washington et al. (2000) have failed to estimate regional ET because of the large size of the area, surface heterogeneity and poor distribution of spatially referenced hydro-climatic data. In this context, Opoku-Duah et al. (2008) proposed remote sensing as a very effective way for modelling evaporative fluxes at the regional scale in the Black Volta Basin.

Surface energy balance systems (SEBS) was developed by Su (2002) for the estimation of atmospheric turbulent fluxes using satellite Earth observation data. It uses remote sensing based approach to estimate evapotranspiration based on surface energy balance equation. SEBS has the ability to estimate ET over large areas and on regional estimations basis other than just point measurements by other conventional methods (Menenti (1984); Bastiaanssen (1995); Su (2002)).

Accurate estimation of ET is a major challenge to hydrologist due to the spatiotemporal variability of the environmental and physical parameters associated with the latent heat fluxes. ET models depend on intensive meteorological information. Uncertainty in measurement and estimation of input parameters increase the uncertainties in ET estimation (Melesse et al., 2009).

1.2. Problem Statement

It has been demonstrated in previous studies such as(Opoku-Duah et al., 2008) and (Su, 2002) that satellite data can be used to significant improvement in the prediction of evapotranspiration at both local and regional scale. Remote sensing based ET estimation uses measurements from both satellite and meteorological stations. The meteorological stations have got site-specific measurements which give data representative of the area they are situated(WMO-No.544, 2003). In order to get measurement covering the whole region and areas outside these stations, extrapolations need to be carried out and conversions need to be done at various scales to enable accurate estimation at various pixel levels.

SEBS requires as input various sets of data which includes both satellite remote sensing data and meteorological data which are measured at these sites by various instruments. Much have been said and documented about the uncertainties and sensitivities of the satellite remote sensing used in calculating ET through SEBS, e.g. (Gibson et al., 2011; Marx et al., 2008; Su, 2002; Tol & Parodi, 2012). These studies have been carried out with specific study areas in perspective.

Opoku-Duah (2007) and Opoku-Duah et al. (2008) reported of deviations in the estimation of regional ET and remote sensing energy fluxes in the Black Volta Basin. In this study the emphasis is on the uncertainty in meteorological data from synoptic stations in the Black Volta Basin of Ghana and its effect on the output actual ET. Measurements taken at these stations include temperature, relative humidity, wind speed and sunshine hours.

In the estimation of ET it is inevitable that model and input data will introduce some uncertainty due to uncertainties in specific remote data, uncertainties in field data, uncertainties in specific model etc.(Gibson et al., 2011). Whatever the model used will be, these uncertainties in the input will propagate towards the output of the calculated ET. In that effect it is required that the uncertainties are identified and analyzed to enable better accurate measurement of ET in the selected catchment.

The focus of this research is therefore to analyse the output uncertainty to SEBS given a range of possible uncertainty in input in situ data. Assessment of this uncertainty will help in the determination the range possible estimates for the actual ET or a value closer to the reality of the Black Volta Basin of Ghana.

1.3. Research Identification

1.3.1. Main Objective

The primary objective of this research is to identify and quantify how the uncertainty in the input meteorological data affects the estimation evapotranspiration (ET) calculated by the Surface Energy Balance Systems (SEBS). The research considers the estimation at regional scale using measurements from selected weather stations and meteorological measurements in the selected catchment.

1.3.2. Specific Objectives

1. Identify the uncertainty in the input meteorological data to SEBS.
2. Quantify uncertainty in SEBS output using Monte Carlo simulation.
3. Assess the difference of ET in wet and dry areas of the selected catchment with regard to measurement uncertainty.

1.3.3. Specific Research Questions

Identify the uncertainty in the input data to SEBS.

1. What are the sources of uncertainty in the SEBS input meteorological data?
2. How are the uncertainties in the input quantified?

Quantify uncertainty in SEBS output using Monte Carlo simulation.

1. How will the uncertainty be propagated?
2. What is the influence of the uncertainty on the SEBS output?

Access the variation of ET in wet and dry areas of the selected catchment with regard to measurement uncertainty.

1. How does the uncertainty differ between measurements stations?
2. How does the uncertainty differ between measurements in wet and dry areas?
3. Which factors contribute to the different uncertainty estimates between wet and dry areas?

1.3.4. Innovation aimed at

The novelty of this thesis is drawn on the uncertainty is in the output of actual ET estimates using SEBS given a possible range of uncertainty for input meteorological data and how actual ET estimates differ in wet and dry areas of the selected catchment.

1.4. Thesis Outline

The thesis consists of seven chapters. The first chapter is the introduction, background of study and problem statement of the research. It describes the essence of using remote sensing to estimate evapotranspiration. The research objective, questions and innovation are all discussed in details in this chapter.

The second chapter describes the area and the data used variables used for the thesis. Three different sets of data are discussed. Detailed description of the data used and their spatial attributes are also discussed.

In chapter three, previous and related works carried out with same methodology are discussed. Chapter four explains the methodology used in the study.

Chapter five is about results whiles chapter six is about discussions drawing on the relevance of the results obtained. Graphs to illustrate results as well any other and explain further distributions of study are showcased in this chapter.

Chapter seven explains the conclusions, recommendations and limitation of the study.

2. STUDY AREA AND DATA DESCRIPTION

2.1. Study area

The Black Volta basin is located in West Africa and has a total area of approximately 155,000 km². It is shared between four countries namely Burkina Faso, Cote d'Ivoire, Ghana and Mali. The portion of the basin lying within the boundaries of Ghana is about 28,000 km² and has a total of four synoptic stations (see Table 2:1). The study area lies between the following coordinates 15.2N, 4.7S, 2.3E, -5.4W in the Black Volta basin (see Figure 2:1).

Station Name	Latitude	Longitude	Elevation Above mean Sea level.(m)
Bole	9.03	-2.48	299.5
Sunyani Airport	7.33	-2.33	308.8
Wa	10.05	-2.50	322.7
Wenchi	7.75	-2.10	338.9

Table 2:1 Weather stations in study area and their coordinates and elevation

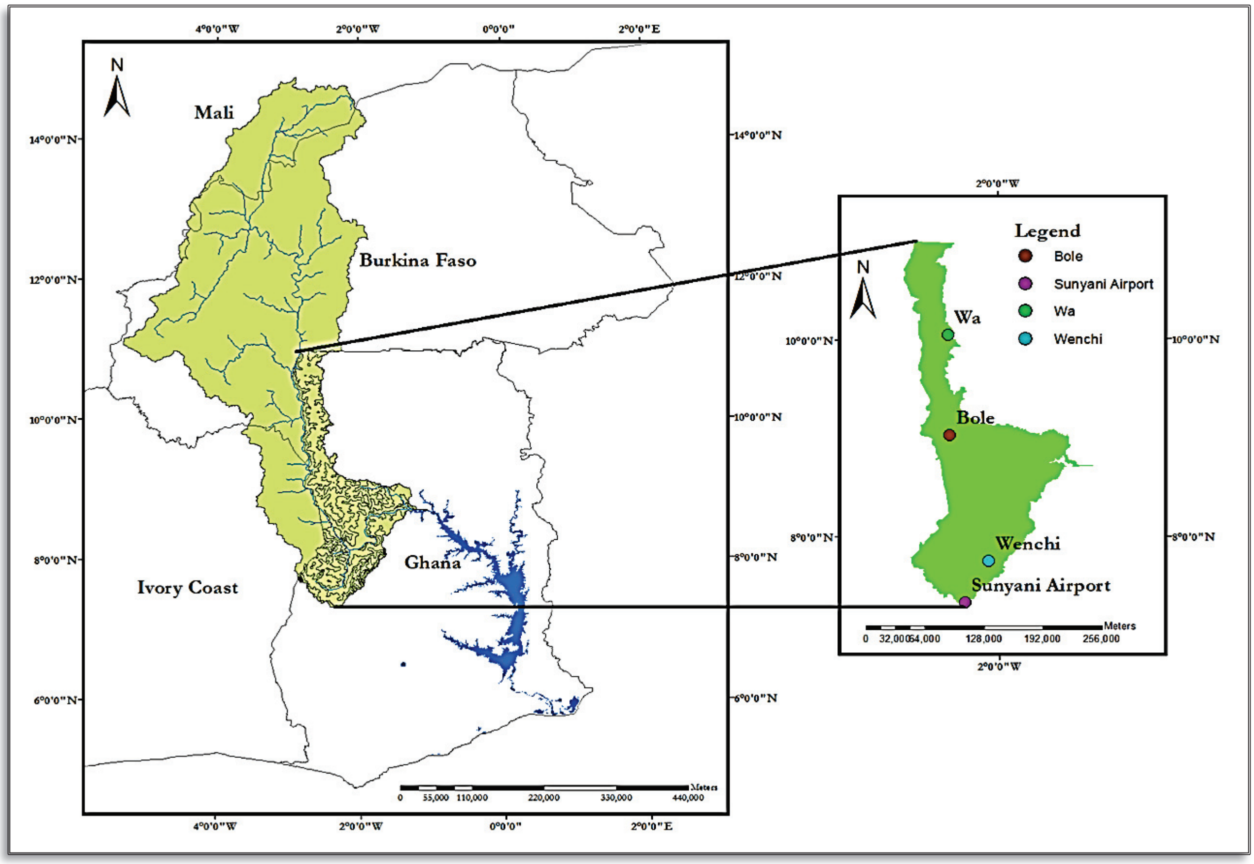

Figure 2:1 Map of study area showing the locations of the four weather stations

2.2. Data Availability

2.2.1. In situ data

The in situ data is collected on daily basis at various meteorological stations by the Ghana meteorological agency. The available data spanned a period of 12 years i.e. Jan/Dec2000-Jan/Dec2011. Some of the stations had some missing data as received from the agency which may be due to malfunctioning of measurement instruments, human errors in data coalition etc.

Table 2:2 shows the data gathered and their temporal resolution. Figure 2:2 shows the annual rainfall for years of collected data. (Data source: Ghana Meteorological Agency (GMA).

Short Name	Product Type and Name	Temporal Resolution
Rainfall	Rainfall (mm)	daily
Tmax and Tmin	Maximum and minimum Temperature(°C)	daily
Wind Speed	Wind Speed (knots)	daily
RH	Relative humidity (%)	daily
Sunshine	Duration of sunshine (hrs.)	daily

Table 2:2 Data collected from weather stations in study area.

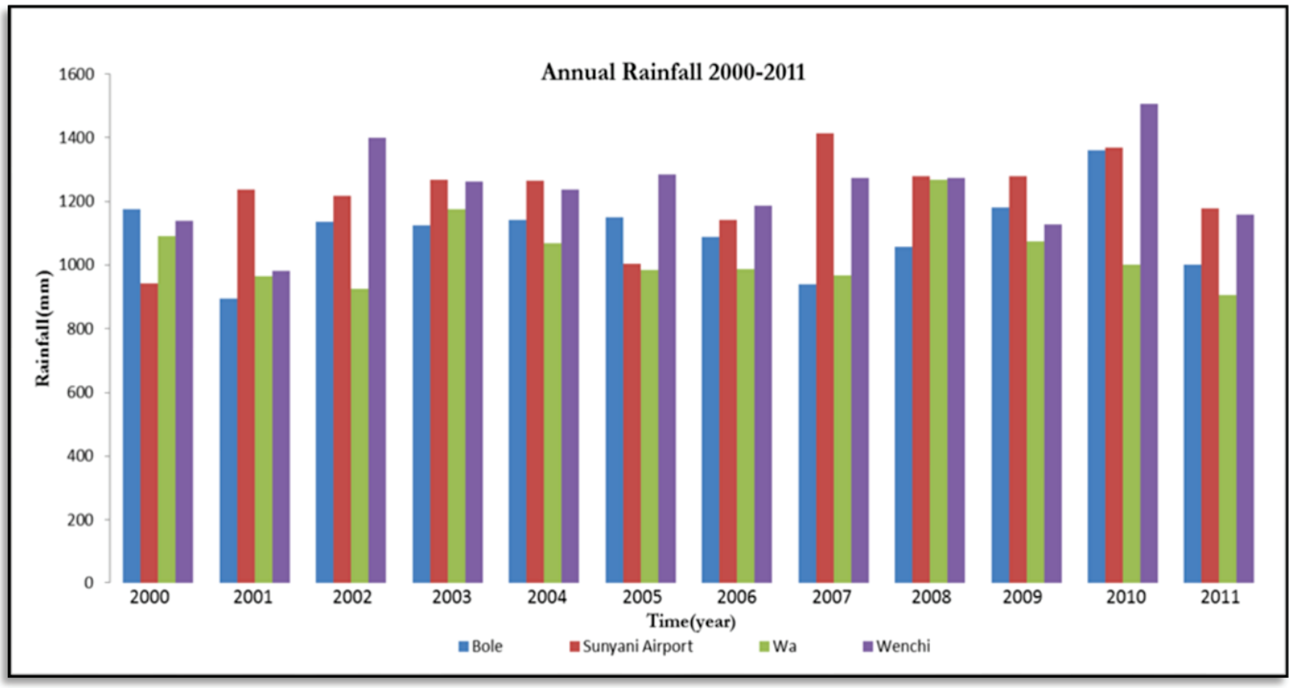

Figure 2:2 Annual rainfall pattern of the study from 2000 to 2011.

2.2.2. MODIS satellite data

The Moderate Resolution Imaging Spectroradiometer (MODIS) is an instrument which operates on both the Terra and Aqua spacecraft with a viewing swath width of 2,330 km viewing the whole surface of the Earth every one to two days. The detectors of MODIS measure in 36 spectral bands, each of them at one of the three spatial resolutions: 250-m, 500-m, or 1,000-m.

MODIS Land products from LP DAAC are distributed at various temporal resolutions, based on the instruments' orbital cycle and the products aggregation level. **S**tandard MODIS Land products use this Sinusoidal grid tiling system which is 10 ° by 10 ° at the equator. They starts at (0, 0) (horizontal tile number, vertical tile number) in the upper left corner and proceeds right (horizontal) and downward (vertical).

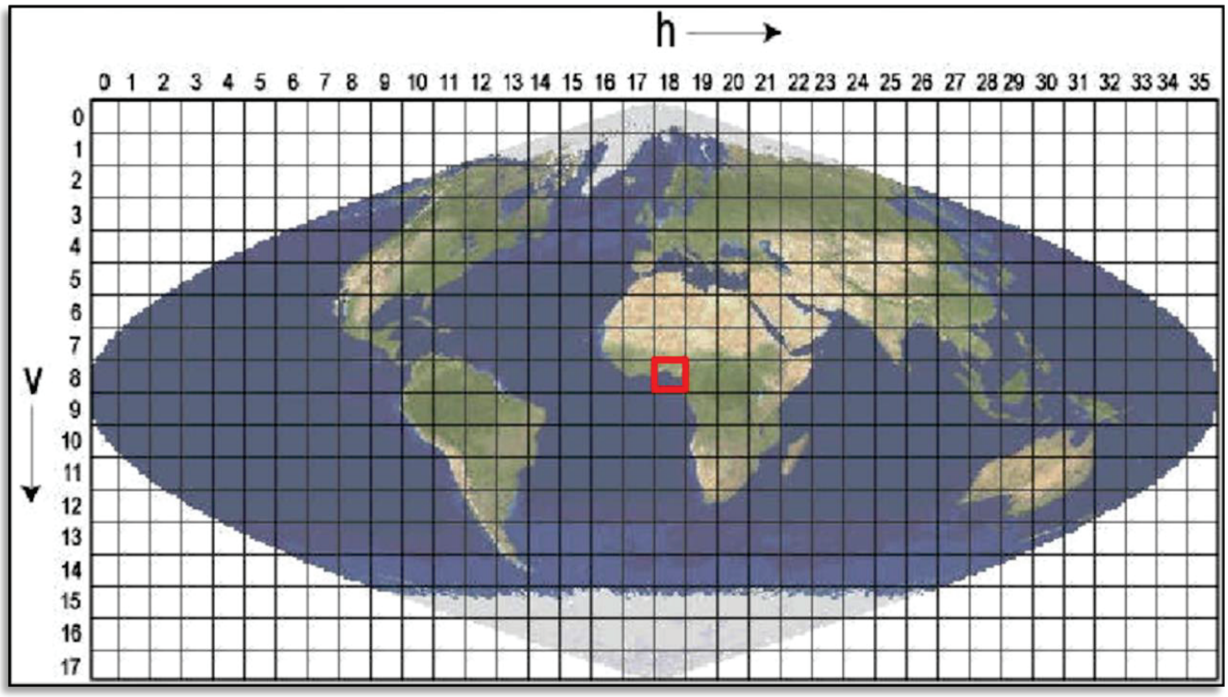

Figure 2:3 MODIS Tiles showing study area in red.
(Source: http://modis-land.gsfc.nasa.gov/MODLAND_grid.html)

MODIS products have two sources of metadata which are the embedded HDF metadata, and the external ECS metadata. The HDF metadata includes global attributes and data set-specific attributes pertaining to the granule. Below is an image showing the tiles where in lies the chosen study area. In this study, MODIS combined products Terra/Aqua pre-processed (see Table 2:3) are used to determine actual evapotranspiration (ETa). The products are downloaded from the site http://e4eil01.cr.usgs.gov:22000/WebAccess/drill?attrib=home&next=group.

SEBS uses remote sensing input data from MODIS namely land surface temperature, emissivity, albedo, NDVI, fraction vegetation cover, land cover map and leaf area index. See appendix C for technical specifications. Table 2:3 shows the MODIS data used for this thesis with their spatial and temporal resolution.

Short Name	Product Type and Name	Spatial Resolution	Temporal Resolution
MOD11A1	Land Surface Temperature/Emissivity L3 Global	1km Grid	Daily
MCD43B3	Combined Albedo L3 Global	1km Grid	16-Day
MOD13A2	Vegetation Indices L3 Global	1km Grid	16-Day
MOD15A2	Leaf Area Index L4 Global	1km Grid	8-Day
MCD12Q1	Land Cover Type L3 Global	500m Grid	Yearly

Table 2:3 MODIS products used in this study.

2.2.3. ECMWF meteorological data

The European Centre for Medium-Range Weather Forecasts (ECMWF) real-time products is available in FM92 GRIB code or in other forms subject to local availability. Forecast parameters are available at 3-hourly intervals up to +144 hours and at 6-hourly intervals from +145 to +240 hours based on 00 and 12 UTC high-resolution forecasts and the Ensemble Prediction System (EPS). ECMWF forecast products can be retrieved at a wide range of spatial resolutions, from regular and rotated lat-lon grids to the original regular and reduced Gaussian grid.

The data can be retrieved from model, pressure, isentropic or iso-potential vorticity (PV) levels, depending on the parameter. Temperature, wind and geopotential forecast information is stored in spectral components but can be interpolated to a specified latitude-longitude grid. This interpolation can also be applied to near surface parameters, although direct use of the original reduced Gaussian grid point values is strongly recommended, especially for precipitation and other surface fluxes.

Table 2:4 shows the ECMWF data used with their spatial and temporal resolution.

(http://www.ecmwf.int/products/forecasts/guide/Temporal_retrieval.html).

Short Name	Product Type and Name	Spatial Resolution	Temporal Resolution
Ta	2 m temperature	global grid	0:00 and 18:00 UTC, 6hourly
Habl	Boundary layer height	global grid	0:00 and 18:00 UTC, Only at 0.00 and 12.00
Ps	Surface pressure	global grid	0:00 and 18:00 UTC, 6hourly
Rin_s	Surface solar radiation downwards	global grid	0:00 and 18:00 UTC, Only at 0.00 and 12.00
Rin_t	Surface thermal radiation downward	global grid	0:00 and 18:00 UTC, Only at 0.00 and 12.00
Tdew	2 m dew point temperature	global grid	0:00 and 18:00 UTC, 6hourly
P0	Mean sea level pressure	global grid	0:00 and 18:00 UTC, 6hourly

Table 2:4 ECMWF real-time products used in the study

(Source: http://ecmwf.int/products/data/)

2.3. Summary

The Black Volta Basin which is shared between four countries namely Burkina Faso, Cote d'Ivoire, Ghana and Mali has four observed meteorological stations in the part that lies in Ghana. Two of these stations Bole and Wa are in the dry region of the basin and the other two Sunyani airport and Wenchi are located in the forest belt. In relation to this study, to calculate the evapotranspiration using the SEBS algorithm three sets of data are used. The meteorological data set gathered by the Ghana Meteorological Agency, the MODIS data which is satellite based and the ECMWF data which is a modelled meteorological data.

3. LITERATURE REVIEW

3.1. Evapotranspiration (ET)

"There is no global, validated ET product available today. We can find products of other components of the terrestrial water cycle, like rainfall and soil moisture, but not of ET. This means that remote estimation of ET is custom made, and that it requires specific skills", (Van der Tol and Parodi 2012) InTech, 2012 pp227. One underlying problem with ET estimation is that, it cannot be measured directly. ET affects the energy and water balance e.g. evapotranspiration reduces soil moisture content and cools the land surface, (Tol & Parodi, 2012).

Gyau-Boakye and Tumbulto (2000) demonstrated that there has been a decline of rainfall in most areas of the Volta basin since 1970. This has resulted in reduction of stream flows of some catchments by 23.1% - 32.5%. Paturel et al. (1997) demonstrated that land surface deterioration has significantly contributed to 1% rise in temperature from 1945 till 1993. This has consequently increased the attraction of surrounding air for atmospheric water vapour by approximately 5-6%, thus, increasing regional evapotranspiration losses (Gyau-Boakye & Tumbulto, 2000). The overall effect is decline in lake levels at e.g., the Akosombo dam site leading to massive hydro-electric power rationing for most of the years.

Many attempts have been taken in recent years to determine the spatial distribution and temporal variability of actual evapotranspiration either through measurements or modeling approach. Examples of such are Bastiaanssen et al. (1998), Su (2002) and many more. Remote sensing approach has been used in various ways to determine ET. The accuracy of the remote sensing approach in the estimation of ET at particular satellite overpass time is restricted to situations with no cloud cover. These restrictions make the remote sensing approach not practical in most mid-latitude climates, especially the tropical regions (Oguntunde, 2004).

In the paper by Opoku-Duah et al. (2008), he compared evapotranspiration over the savannah part of the Volta Basin in West Africa. Using remotely sensed data, he explained the relevance of the spatial dynamics of evapotranspiration (ET) as an important attribute for food security and water resources management in Africa. Opoku-Duah et al. (2008)also elaborated on the importance of accurately estimating evapotranspiration using remote sensing method to overcome the problem of spatial variability at the regional scale. It went further to emphasize that "over- or underestimation of ET can provide misleading information required for water policy decision-making and resource allocation".

Opoku-Duah (2007) showed in derivation of energy and water balance parameters from ENVISAT AATSR data an error margin of approximately 2.0 mm day^{-1} when the AATSR was compared with ground ET observations. These observed differences may be due to differences in sensor calibration and spatial mismatch between satellite and ground observations. ET is a critical variable in in our natural environment and such there is the need to estimate or model it using observed meteorological variables, (Oguntunde, 2004).

3.2. Surface Energy Balance Systems (SEBS)

Estimation of atmospheric fluxes has been estimated by research works such as Su (2001) using SEBS with satellite Earth observations of the parameters of the energy fluxes. SEBS is based on the determination of land surface physical parameters which includes albedo, emissivity, temperature, vegetation cover, leaf area index and many more from spectral reflectance and radiance. SEBS can be used at both local scale and regional scale under all stable atmospheric conditions (Su, 2006).

Using SEBS, Jia et al. (2003) have successfully modeled forecast fields of the large scale numerical weather prediction (NWP) model to radiometric measurements from the Along Track Scanning Radiometer (ATSR) onboard the European Remote Sensing Satellite (ERS-2). SEBS was also used by Rauwerda et al. (2002), for parallel-source model which showed significant improvement in estimated turbulent heat fluxes. Other authors such as Li (2001), Su et al. (2003a), Su et al. (2003b) have used SEBS to generate daily, monthly and annual ET in semi-arid areas and also for drought monitoring as well as estimating atmospheric fluxes. SEBS has proven to be reliable and acceptable in estimating turbulent fluxes and evaporative fraction at different scales. Idso et al. (1975) and Shukla and Mintz (1982), emphasized the fact that regional ET from land surface is essential to understand water cycle, and to estimate surface runoff and groundwater. A demonstration of the schematic representation of SEBS as shown by Su in the encyclopaedia of hydrology is shown in Figure 3:1.

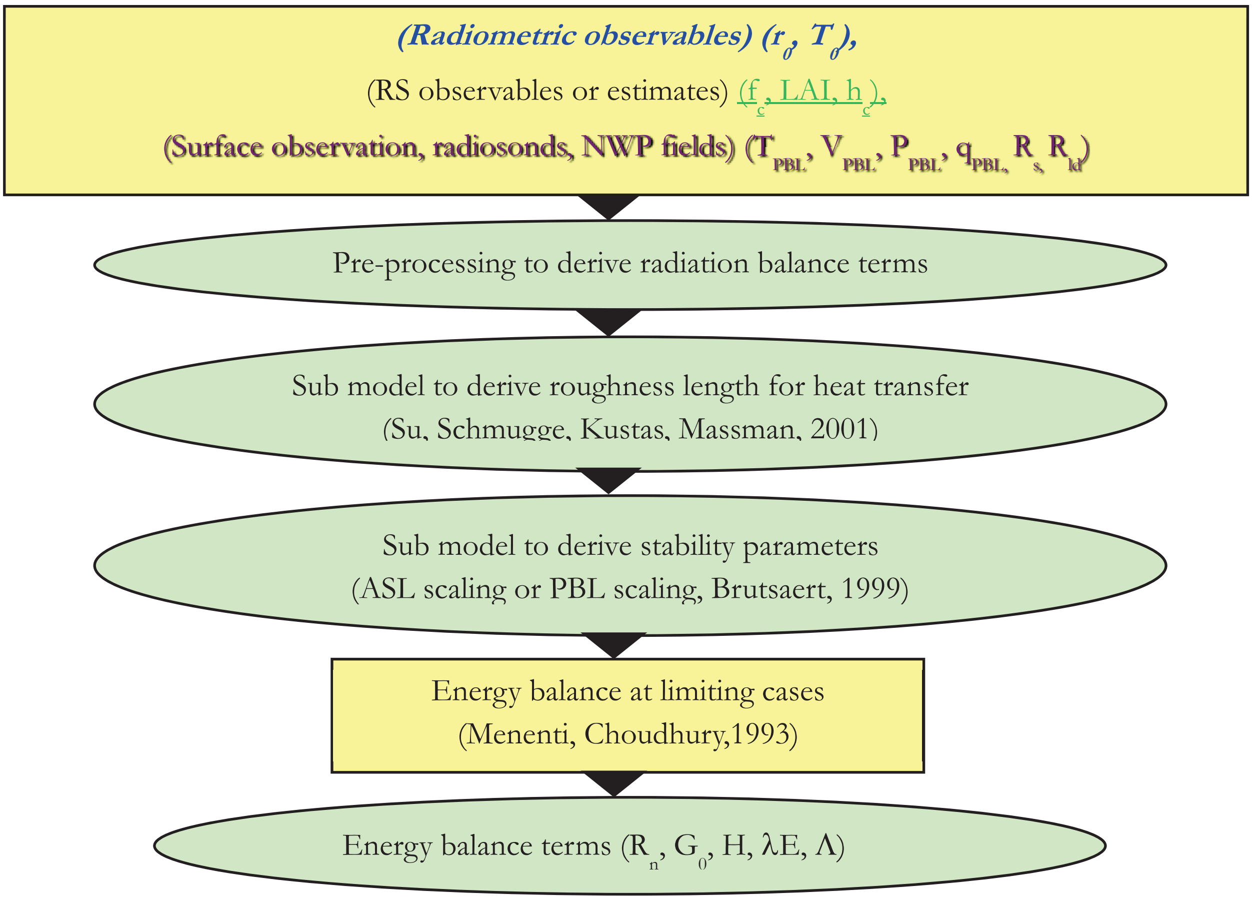

Figure 3:1. Schematic representation of SEBS. (Su, 2006)
Encyclopedia of Hydrological sciences, pp. 740.

3.3. Uncertainties in SEBS/Remote Sensing ET estimates

Many a times has researchers reported of uncertainties in measures used in estimating the actual evapotranspiration either through remote sensing approach or other. Allen et al. (2011) elaborated on the uncertainties accompanied by evapotranspiration measurements which include systematic error associated with sensor calibration bias, improper sensor function, improper sensor operation, improper sensor placement, inaccurate sensor recording, inadequate or incorrect model associated with data interpretation or processing, unrepresentative vegetation characteristics, improper data reduction procedures, and improper use of time step integration. But on the other hand they stated that since there are wide ranges in types of error and causes for error in ET measurements, it is difficult to assign estimates for average error associated with any particular type of measurement system.

Uncertainties in SEBS and other remote sensing based estimates of ET can be grouped according to errors in input data, uncertainties related to spatial heterogeneity of the study area, resolution of input data and processing errors resulting in either error production or error propagation or both (Gibson et al., 2010). These uncertainties and possible errors are accumulated as the SEBS model for calculating ET has a complex process which needs several image processing steps to produce the final result.

There is large uncertainty in deriving latent heat which extends to the estimation of evaporative fraction. Meteorological variables such as surface temperature have uncertainty whose propagated effect in latent heat cannot be avoided Su (2006). SEBS accurately estimates sensible heat provided the variables used are accurate to within 50% of their true value Su (2002).

There are difficulties that come with the use of remote sensing to acquire the temporal and spatial variation in surface fluxes. Regardless of all these difficulties, satellites are the only capable ways to estimating relatively small-scale variations, over regional domains and on a regular basis. There is the ability to examine multiple spatial resolutions from various Earth observation sensors in the wake of limitations of better high-resolution characterization of surface fluxes, in the temporal domain, due to lack of platforms (McCabe & Wood, 2006).

Van der Kwast et al. (2009) used distributed field measurements of sensible heat flux to evaluate SEBS at landscape scale. It was realized that SEBS is viable of estimating H in the magnitude scale as filed measurements. Standard deviations in field measurements of sensible heat flux are similar to standard deviations of modeled sensible heat flux by SEBS. In a well irrigated area, SEBS estimated sensible heat can deviate by up to 70% when there is 0.5K difference in surface temperature. "Although sensitivity of SEBS derived sensible heat flux to errors in surface aerodynamic parameters is smaller compared to surface temperature, the errors in the estimation of these parameters from remote sensing images using empirical relations can be larger and exceed the 50% limit of input accuracy for many land cover types" (Van der Kwast et al., 2009).

Gibson et al. (2010) encountered various sources of uncertainty in remote sensing ET estimates in his article "Uncertainties in using remote sensing for water use determination: a case study in a heterogeneous study area in South Africa" which were classified as

1. errors in input data;
2. uncertainties related to spatial heterogeneity of the study area and resolution of input data;
3. processing errors resulting in either error production or error propagation or both.

Gibson et al. (2010) went further to describe some of these uncertainties by example of the estimation of ET using SEBS. Input data related uncertainty, heterogeneity of study area related uncertainty and data processing uncertainty were all demonstrated in this paper using land surface and air temperature, land cover and topography and fraction vegetation cover as examples. These uncertainties and potential errors are accumulated due to the fact that SEBS is a complex process which requires a lot of different image processing steps combined together to produce the final calculation of ET. Errors are propagated and accumulated through the processing chain, thereby affecting the final output product (Gibson et al., 2010).

Mostl remote sensing algorithms for estimating ET use the energy balance equation. Latent heat is calculated as a residual of the energy balance. Net radiation is easily estimated from remote sensing products and ground heat flux is retrieved from geostationary satellites for sparsely vegetated areas and /or bare land.

Sensible heat is the most critical in the energy balance; both temperature difference and aerodynamics resistance need careful attention (Tol & Parodi, 2012).

Tol and Parodi (2012)went further to explain that:

1. there's the need to use local lapse rates to do temperature correction in areas of high elevation difference as the errors in temperature are normally so high;
2. the accuracy of temperature gradient should be better then $2^{o}C$ in order to achieve reasonable results;
3. a two -source model is preferred over a single source model for sparsely vegetation because in the single source model the parametization of roughness length for heat transfer is just a "wild guess".

3.4. Penman Monteith (PM) Equation

Allen et al. (1998)recommends the FAO-PM for daily reference evapotranspiration. Allen et al. (1998) proposes a complete set of equations to compute the parameters according to the available weather data and the time step computation, which constitute the so called FAO-PM method. The reference evapotranspiration (ET_o) rate is attributed to reference surface. The reference surface is a hypothetical grass of 20cm long and not short of water. ET_o is only affected by climatic variable thus ET_o is a climatic parameter and is appropriate to compute it with weather station data. It expresses the evaporating power of the atmosphere at a specific location and time of the year. ET_o does not consider the crop characteristics and soil factor, (Allen et al., 1998).

3.5. Summary

Accurately estimating evapotranspiration helps to make informed decisions in Earth system analysis and hydro climatic sector. Evapotranspiration is estimated by method which includes Penman Montieth and remote sensing techniques such as SEBS. SEBS uses satellite data and filed data to estimate evapotranspiration. Estimation of evapotranspiration comes with uncertainty from different sources which can include model parameterization, input data, sensor orientation etc. and SEBS is not far from it.

4. METHODOLOGY

Identifying the real behaviour of uncertainties resulting from input data is still a challenge and care needs to be taken in its analysis. The uncertain input meteorological variables of SEBS considered in this study are wind speed, sunshine hours and air temperature. For each of these variables a normal probability distribution function (PDF) is specified according to the standard deviations stated WMO-No.8 characterized measurement uncertainty. Figure 4:1 illustrates the series of the in situ data for January 2010.

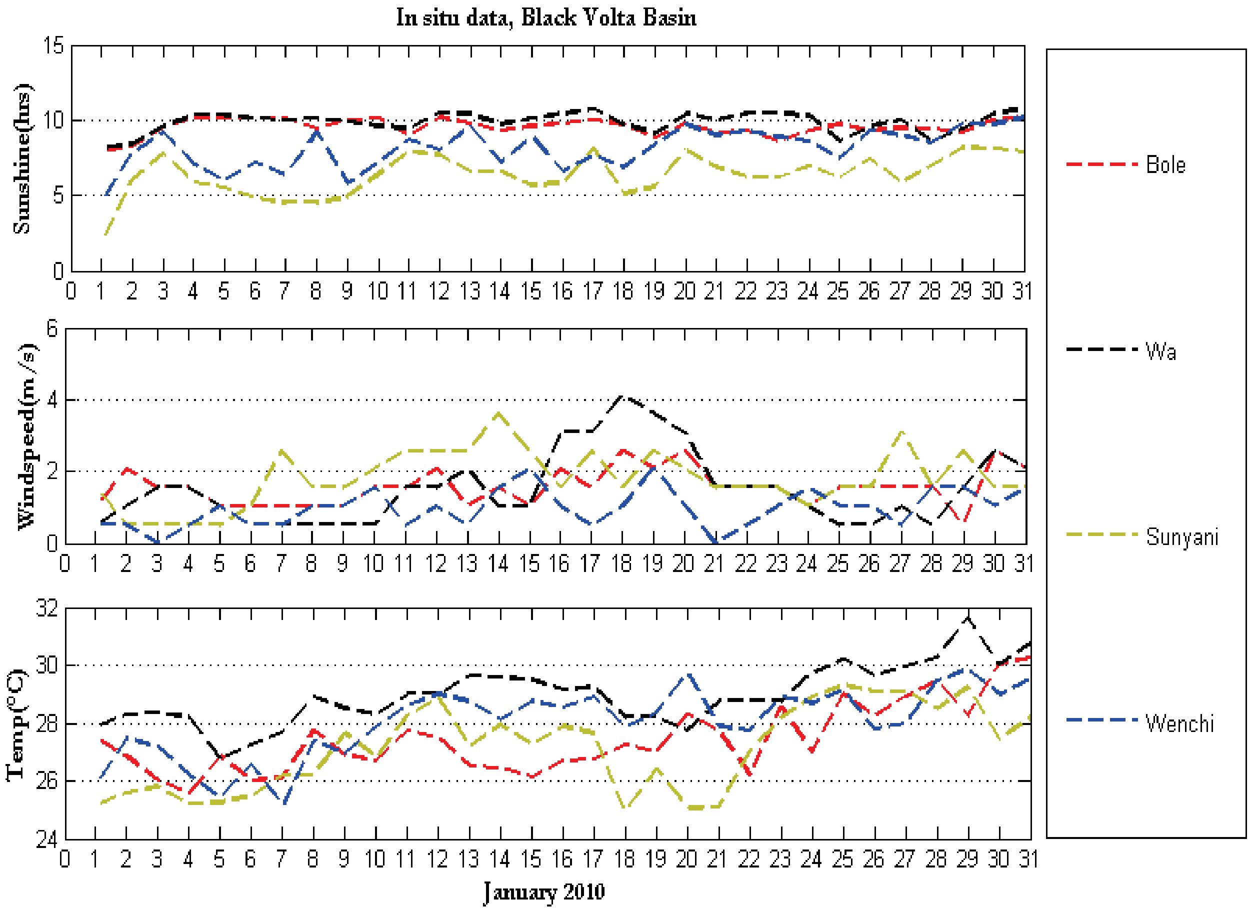

Figure 4:1 In situ data for stations in the Black Volta Basin

The variables (temperature, wind speed and sunshine hours) were used together with other input variables to produce the baseline value of actual evapotranspiration. In this thesis baseline is used in place of true value as we cannot ascertain that the value measured is the true actual ET. The baseline ETa estimate is used as the benchmark for the analysis.

100 simulations were realised using the PDFs (see Table 4:1) of the required uncertainty of these variables with the Monte Carlo simulation method. Each simulation is used to estimate a set ETa values which are then used in comparison with the baseline value to analyse the RMSE which tells how far the simulated value is from the baseline value and how far the input uncertainty affects the output. The final quantified uncertainty is characterized with a histogram, mean, median and standard deviation of the output simulated ETa. Figure 4:2 describes is a flow chart describing the research frame work of the thesis.

4.1. Flow Chart of methodology

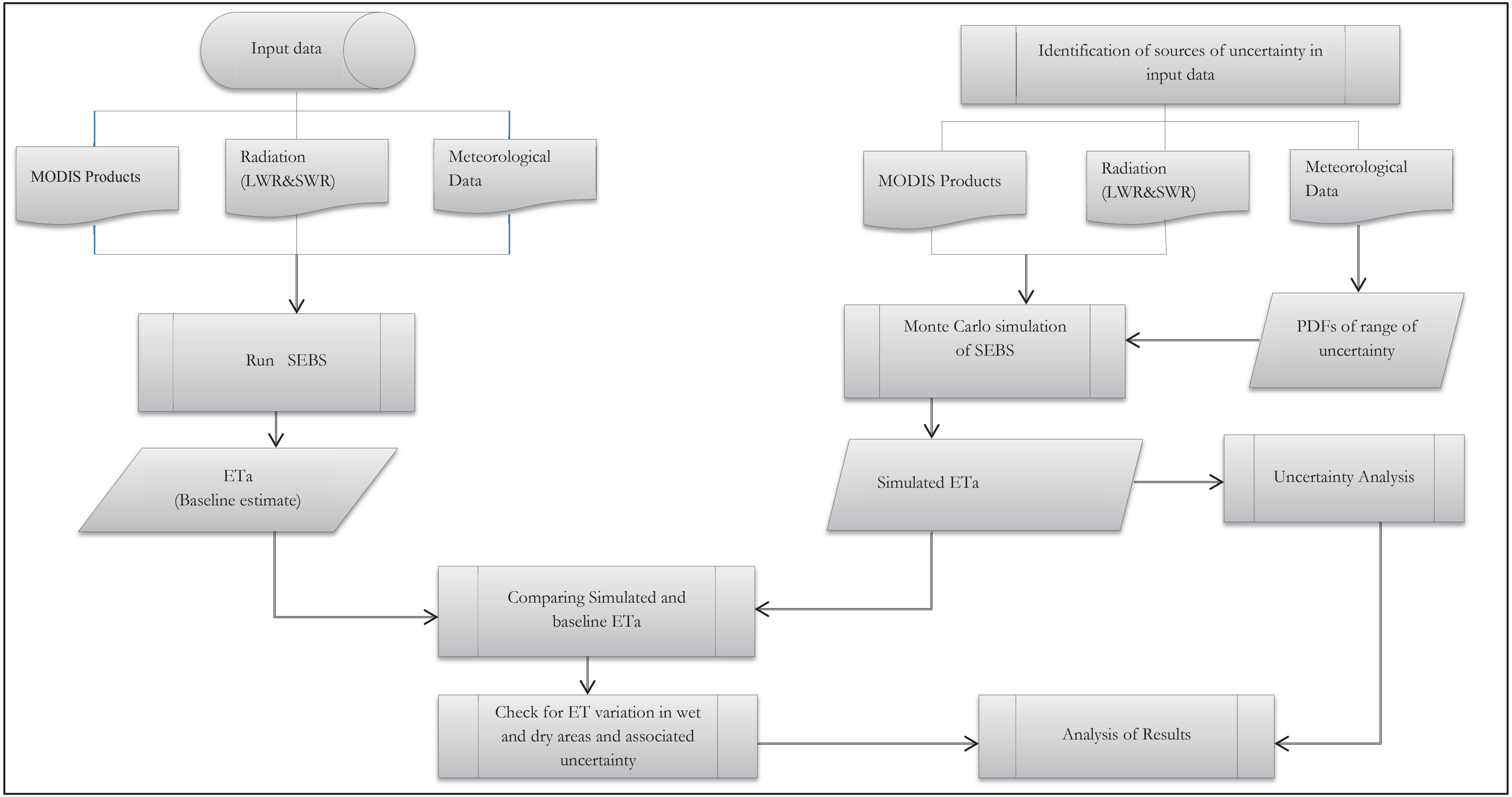

Figure 4:2. Flow Chart of methodology

4.2. Model Description

4.2.1. Surface Energy Balance Systems

SEBS requires an input of three sets of data/information. Land surface temperature, albedo, emissivity, fraction vegetation cover and leaf area index forms the initial set. Normalized Difference Vegetation Index (NDVI) is used when vegetation information is not explicitly available. The initial set of inputs are derived from remotely sensed data (Su, 2002). The next set consist of air pressure, temperature, humidity, wind speed and sunshine hours at reference height. The reference height is the standard measuring height at the weather stations where these measurements are taken also known as the planetary boundary layer. The data set can also be derived from meteoroidal models from European Centre for Medium-Range Weather Forecasts (ECMWF). The third set includes downward solar radiation and downward longwave radiation which can be measured directly or taken from model output from ECMWF. Figure 4.3 illustrates the processes of SEBS, where the second and third input sets together are referred to as a the 'Meteorological Data'

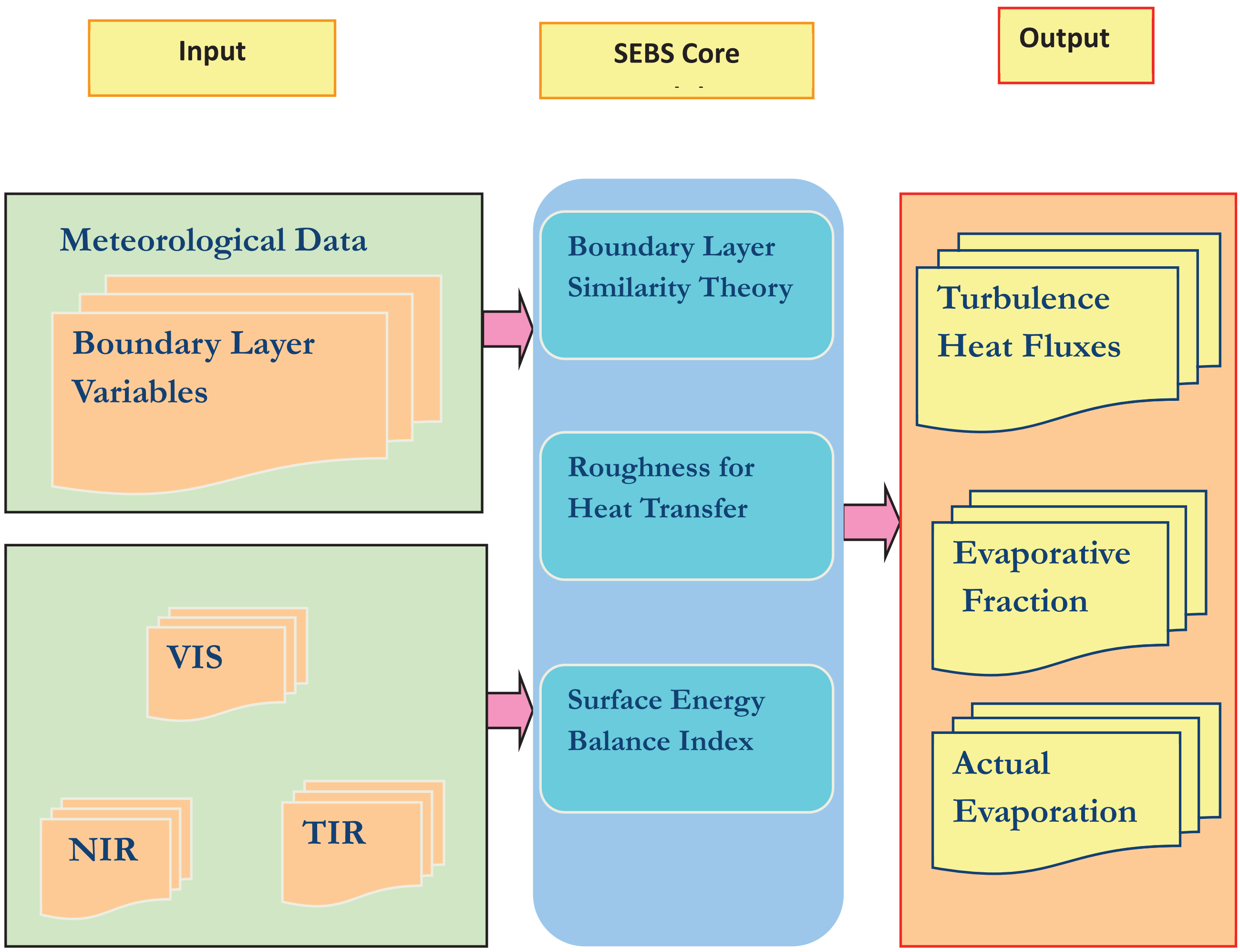

Figure 4:3 Components of the SEBS (Wang et al., 2008)

4.2.2. Surface Energy Balance Equations

The general surface energy balance equation as also used by (Su, 2002)is written as

$$R_n = G_o + H + \lambda E \tag{4.1}$$

Where R_n net radiation G_o is the soil heat flux, H is the sensible heat flux, E is the actual evapotranspiration and λ is the latent heat, λE together makes the turbulent heat flux.

4.2.2.1. Net Radiation equation

$$R_n = (1 - \alpha) \times R_{swd} + \varepsilon \times R_{lwd} - \varepsilon \times \sigma \times T_o^4 \tag{4.2}$$

Where R_{swd} is the downward solar radiation, R_{lwd} is the downward longwave radiation, α is the albedo ε is the emissivity of the surface, T_o is the surface temperature and σ is the Stephan-Boltzmann constant.

4.2.2.2. Soil heat flux equation

$$G_o = R_n \times [\Gamma_c + (1 - f_c) \times (\Gamma_c - \Gamma_s)] \tag{4.3}$$

It is assumed that the ratio of soil heat flux to net radiation is $\Gamma_c = 0.05$ for full vegetation canopy (Monteith, 1973) and $\Gamma_s = 0.315$ for bare soil, (Kustas & Daughtry, 1989) cited in (Su, 2002). A weighted average is calculated for each pixel from these values according to the fraction of the vegetation cover (f_c).

4.2.2.3. Sensible Heat flux equation

The sensible heat flux (H) can be defined as the exchange of heat through air as results of temperature gradient between the surface and the atmosphere, (Tol & Parodi, 2012).

$$H = \rho_a \times C_P \times (T_{o-} T_a)/\Upsilon_{ah} \tag{4.4}$$

Where ρ_a the density of moist air C_P is the air specific heat at constant pressure Υ_{ah} is the aerodynamic resistance to heat transport between the surface and the reference level and T_o is the surface temperature and T_a is the temperature at reference height.

4.2.2.4. Latent heat flux

Latent heat flux is calculated as a residual of the energy balance. Since H, G_o and R_n are instantaneous measurements, it is important to find a procedure to integrate to daily totals. The model makes use of the evaporative fraction Λ. It is the energy used for the evaporation process divided by the total amount of energy available for the evaporation process, (Brutsaert & Sugita, 1992) cited in (Tol & Parodi, 2012)

$$\Lambda = \lambda E / (\lambda E + H) = \Lambda_r \times \lambda E / (R_n - G_o) \qquad (4.5)$$

Λ_r is the relative evaporation. Evaporative fraction is assumed to remain constant throughout the day.

$$E_{DAILY} = ((8.64 \times 107 \times \Lambda_{24hrs})/\lambda\rho_w) \times R_{n,24hrs} \qquad (4.6)$$

Where λ = 2.0501- 0.00.236 $\times$ T_a MJ kg^{-1}, ρ_w= 1000 kg^{-3} and $R_{n,24hrs}$ is the average net radiation over 24 hours $[Wm^{-2}]$ and E_{DAILY} is the daily actual evapotranspiration.
See extra formulae in appendix B.

4.2.3. Reference ET estimation by Penman Monteith Method

Reference daily evapotranspiration is estimated using Penman-Monteith method. Data from stations Bole, Sunyani Airport, Wa and Wenchi collected from the Ghana Meteorological Agency was used to calculate evapotranspiration together with required inputs for ET_o.

For this estimation various meteorological variables are required as inputs. These include solar radiation, temperature (maximum and minimum), wind speed and relative humidity. These variables may include some random as well systematic errors that may account for inaccurate ET output. Nevertheless the main aim of this potential ET output is to compare to the baseline estimate of actual ET in order to assess the trend in the selected catchment for the year 2010.

$$ET_o = \frac{0.408\Delta\,(R_n - G) + \Upsilon\,(900/\,(T + 273))\,u_2\,(e_s - e_a)}{\Delta + \Upsilon\,(1 + 0.34\,u_2)} \tag{4.7}$$

Where

ET_o = reference evapotranspiration, $\mathrm{mmday^{-1}}$;

R_n = net radiation at the crop surface, $\mathrm{MJ\ m^{-2}\ d^{-1}}$;

G =soil heat flux density, $\mathrm{MJ\ m^{-2}\ d^{-1}}$;

T =Air temperature at 2 m height, $^{\mathrm{o}}\mathrm{C}$;

u_2 =wind speed at 2 m height, $\mathrm{ms^{-1}}$;

e_s = saturation vapor pressure, kPa;

e_a = actual vapour pressure, kPa;

$e_s - e_a$ = saturation vapour pressure deficit, kPa;

Δ =slope of the vapor pressure curve, kPa$^{\mathrm{o}}\mathrm{C}^{-1}$;

Υ = psychrometric constant, kPa$^{\mathrm{o}}\mathrm{C}^{-1}$.

Required inputs for ET_o calculation

$Tmax$	Maximum temperature ($^{\mathrm{o}}\mathrm{C}$)
$Tmin$	Minimum temperature ($^{\mathrm{o}}\mathrm{C}$)
$RHmax$	Maximum relative humidity (%)
$RHmin$	Minimum relative humidity (%)
R_s	Average solar radiation ($\mathrm{MJ\ m^{-2}\ d^{-1}}$;)
u_2	Average wind speed ($\mathrm{ms^{-1}}$at $\mathrm{h^b}$ m)
P	Atmospheric pressure (barometric) kPa
z	Site elevation above sea level (m)
J	Julian day -
LAT	Latitude degree

See appendix A for results

4.2.4. Monte Carlo Simulation for Uncertainty evaluation

Monte Carlo Simulation is a technique that uses sets of random number generation and probability to solve problems. The "Guide to expression of uncertainty measurement (GUM)"(JCGM:101, 2008) and (BIPM et al., 2008) expresses the various steps used in uncertainty evaluation as in three stages namely formulation, propagation and summarizing. JCGM:101 (2008) gives makes provision for applying Monte Carlo and gives guidance for Monte Carlo Simulation in meteorological applications.

The formulation process takes the following steps

1. Defining the output quantity Y,
2. Determination of input quantities $X = (X_1, \ldots \ldots X_N)^T$
3. Develop a model for Y and X
4. Assign probability distribution functions (PDFs) to the X_i
5. Propagate the PDFs for the X_i through the model to obtain the PDF for Y and finally summarize using the PDF for Y.

Summarizing, use the PDF for Y to obtain:

1. The expectation of Y , taken as an estimate y of the quantity.
2. The standard deviation of Y , taken as the standard uncertainty $u(y)$ associated with y as expressed in (JCGM:101, 2008) and (BIPM et al., 2008)
3. The mean, median, percentiles and interquartile ranges are also produced in this thesis.
4. A coverage interval containing Y with a specified probability (the coverage probability).

Figure 4:4 illustrates the idea of using PDFs in uncertainty propagation

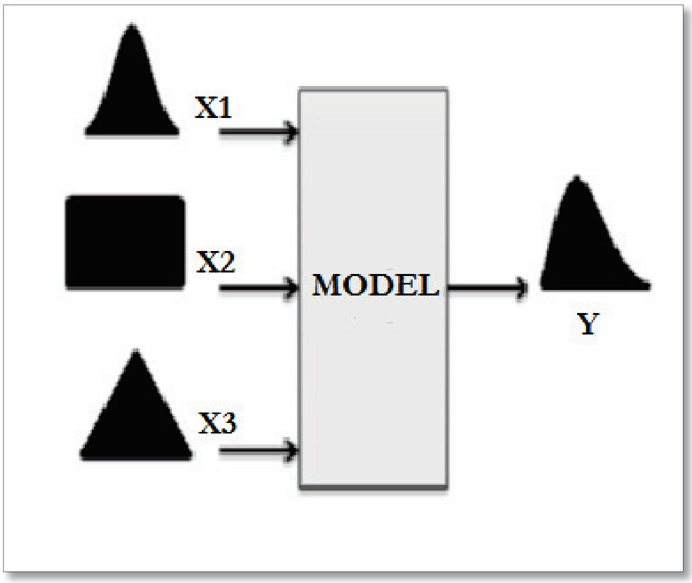

Figure 4:4 Illustration of uncertainty propagation with PDFs

Monte Carlo Simulation approach has been used by various authors to evaluate uncertainty. To mention a few, Ángeles Herrador and González (2004), Decker et al. (2011) and Horne et al. (2012).
This same procedure is embedded in this thesis as it looks at the measurement uncertainty in SEBS taking account the variables from four specific synoptic stations namely Bole, Wa, Sunyani and Wenchi. The variables which are temperature, wind speed and sunshine hours have measurement uncertainty stated in (WMO-No.8, 2008) as PDFs

The approach for evaluating uncertainty in this thesis can there is summarized as follows based on the GUM uncertainty guidelines given in previous page.

1. Establishing the model equation for the measurement process of the individual parameters or input quantities. In this instance the Surface Energy Balance for calculating actual evapotranspiration with particular emphasis daily actual ET(equations 4.1 to 4.6)
2. Identifying the significant sources of uncertainty through analogous approach, in this regard emphasis was placed on the input data measured from ground meteorological stations of the selected study area.
3. Selection of the probability density functions of the selected uncertainty sources. This was done with reference to the WMO guide to meteorological instruments and methods observation((WMO-No.8, 2008) . According to the WMO document the stated measurement uncertainty corresponds to the uncertainty of the true value with a stated probability level 95 per cent a normal distribution.
4. Monte Carlo runs to create samples of input data sets.
5. Execution of the simulations corresponding to the N samples of each uncertainty source.
6. Computation of results of the selected samples for each variable.

   A combined uncertainty $U(y)$ is the calculated as a standard deviation(Ángeles Herrador & González, 2004):

$$U(y) = \sqrt{\frac{\sum_{i=1}^{N}(X_i - \bar{X})^2}{N-1}} \tag{4.9}$$

(4.8)

Further details of the Monte Carlo explanation and output statistics can be seen in (JCGM:101, 2008) .

The mean

$$\bar{X} = \frac{1}{N}\sum_{i=1}^{N} X_i \tag{4.9}$$

4.3. Identification of significant uncertainty sources

Obtaining the true value of a variable is difficult in meteorology as also stated by (Linacre, 1992). Uncertainty of measurements according WMO is the variable associated with the result of a measurement that characterizes the dispersion of the values that could be reasonably attributed to the measured value. Uncertainty of measurement may comprise of many components some of which may be derived from a statistical distribution of a series of measurements and can be characterized by experimental standard deviation, others are evaluated from assumed probability distributions based on experience or literature information. (WMO-No.8, 2008)

For the purpose of this thesis three meteorological variables are being investigated for uncertainty taking into accounts the WMO document required measurement uncertainty. These requirements can be applied to both manned and automatic weather stations as defined in the (WMO-No.544, 2003) document. Table 4:1 shows the three meteorological variables under investigation and their required measurement uncertainty.

Input Variable	Measurement Unit	Product type	Uncertainty
Air Temperature	^{0}C	Meteorological (in-situ)	±0.3 SD
Wind Speed	m/s	Meteorological (in-situ)	±0.5 SD
Sunshine hours	Hrs.	Meteorological (in-situ)	±0.1 SD

Table 4:1. Meteorological variables and their required uncertainty

The stated required measurement uncertainty is the uncertainty of the reported value with respect to the true value and signifies the interval in which the true value lies with a stated probability. The recommended level of probability is 95 per cent for normal (Gaussian) distribution of the variable. It is assumed that when known corrections are taken into consideration, the errors in reported true values will have a mean value close to zero (WMO-No.8, 2008).

4.4. Probability density functions of the selected uncertainty sources and simulations.

As stated in section 4.3 a normal probability density function was selected for the selected sources of uncertainty. A randomly generated uncertainty distribution was generated with the required values stated in Table 4:1for each of the meteorological variables. 100 independent realisation were the generated with the measured in situ data of these meteorological variables.

4.5. Standard error of the mean

The standard error of the mean is used to indicate the variability in the estimate of the mean.
In the context of this work, it is used to check variable of the estimate of the simulated ETa mean.
Assume standard error about the mean to be SE_m then

$$SE_m = \frac{s}{\sqrt{N}} \tag{4.10}$$

Where s the sample standard deviation and N is the sample size

4.6. Calculating the confidence Interval

The standard and means of each simulation per day are computed for each sample per day. The 95% confidence interval for daily ETa values can then be estimated as follows. $Z_{.95}$ is the number of standard deviations extending from the mean of a normal distribution required to contain 0.95 of the area.
$Z_{.95} = 1.96$

95% upper confidence limit = Mean + $Z_{.95} \times SE_m$ (4.11)

95% upper confidence limit = Mean - Z.95 $\times$ SE_m (4.12)

The mean is the daily simulated mean ETa.

It can therefore be stated that the true mean lies somewhere between the upper confidence limit and the lower confidence limit with 95% confidence. In this work, much importance is placed on the overall daily uncertainty spread. Prominence is therefore given to the daily standard deviation which explains more about the precision. High standard deviation constitutes low precision.

4.7. Mean error (ME)

The mean error is used to check for bias in the set of simulated measurements. Consistent negative mean error depicts underestimation of the value being estimated and consistent positive mean error depicts overestimation. When the simulated estimates are consistently larger or smaller than the baseline estimate then it assumed that they biased.

The ME is given as

$$\mathrm{ME} = \frac{\sum_{i=1}^{N}(X_i - Z_i)}{N} \tag{4.13}$$

Where X_i are the simulated estimates, Z_i the baseline estimate and N is the sample size

4.8. Root mean square error (RMSE)

The root mean square error is used to check how far on average the simulated ETa estimates are from the baseline ETa estimated.

It is given

$$\mathrm{RMSE} = \sqrt{\frac{\sum_{i=1}^{N}(X_i - Z_i)}{N}} \tag{4.14}$$

Where X_i are the simulated estimates, Z_i the baseline estimate and N is the sample size

4.9. Summary

SEBS based estimation of evapotranspiration was introduced by (Su, 2002). Uncertainty analysis evapotranspiration estimate based on the SEBS algorithm is carried out using Monte Carlo uncertainty analysis. Output of the Monte Carlo is analysed and assessed for uncertainty. The standard uncertainty is given as the standard deviation of the simulated. Mean, median, mean errors, RMSE, interquartile ranges, percentiles and confidence interval are evaluated thoroughly.

5. RESULTS

This section presents the estimation of actual evapotranspiration (ETa) from both the baseline estimates and the simulated independent samples. Results of uncertainty in the measurements are also presented. Estimates in dry and wet areas of the study region are compared to check for their variability. Variation of actual ET in comparison with potential ET estimated from data in the individual stations of the study area is also analysed.

5.1. Estimation of ETa for meteorological stations in the Black Volta basin of Ghana

Actual ET was estimated with the SEBS equation for the year 2010. Implementation of SEBS was done in MATLAB (Code provided by Dr. Joris Timmermans). The year experienced considerable amount of rainfall which caused flooding mostly in parts of the capital city Accra which does not fall within the study area. But looking at the amount of rainfall that characterized the country as a whole, it brings particular interest to this research to check on how evapotranspiration in other parts of the area look like.
Due to cloud cover, especially in the rainy season, SEBS provided ET estimates for most of the dry area areas and mostly in the dry season.

Sunyani and Bole recorded 6.83 mm of annual maximum ETa in the year 2010 while Wenchi and Wa recorded 6.77mm and 7.04 mm respectively. Figure 5:1 illustrates the estimation of ETa across the year 2010 for the four synoptic stations in the Black Volta Basin of Ghana. Figure 5:2 shows images of ET maps for selected days in both dry and wet seasons.

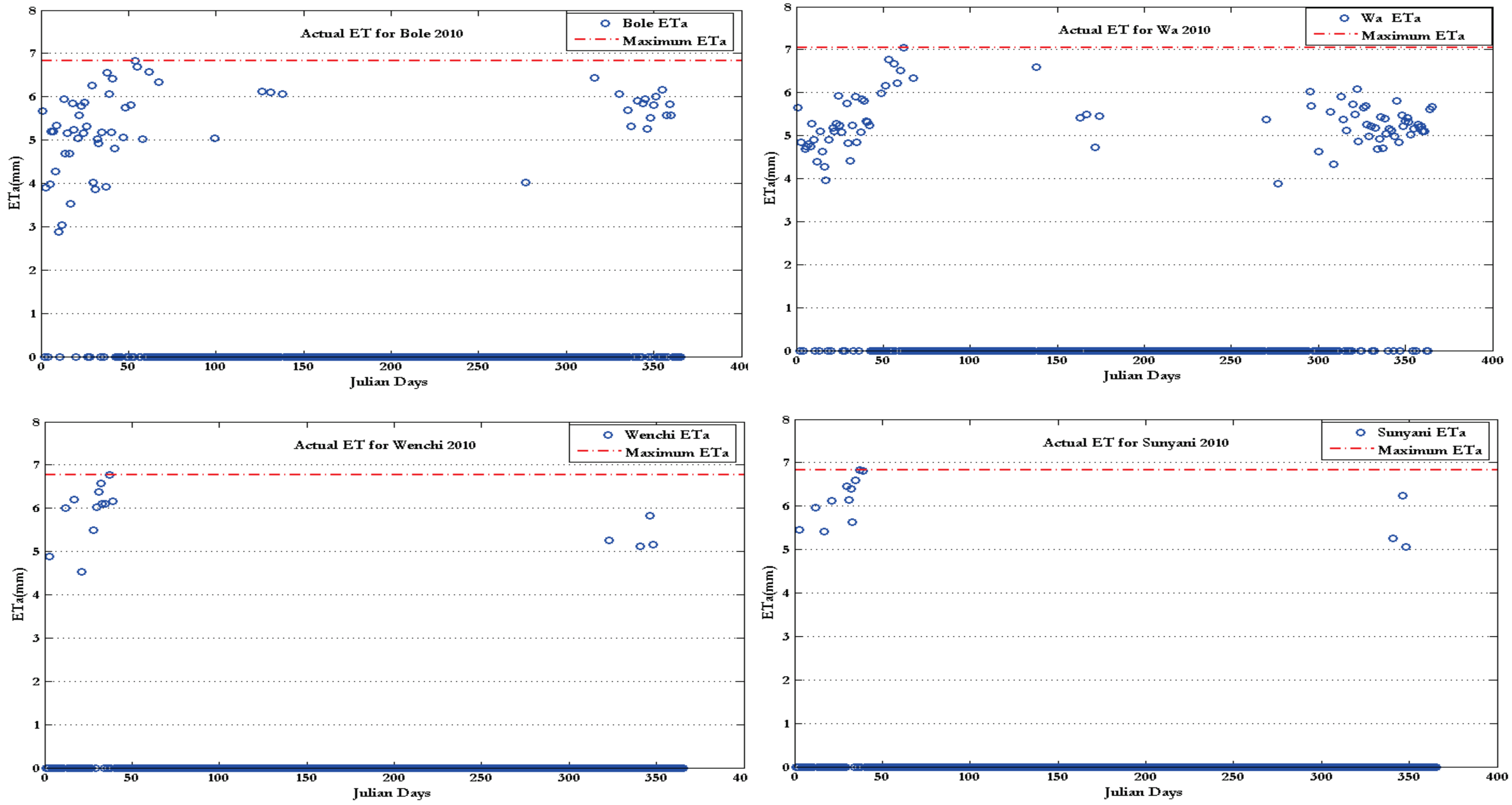

Figure 5:1 Actual Evapotranspiration for the year 2010.

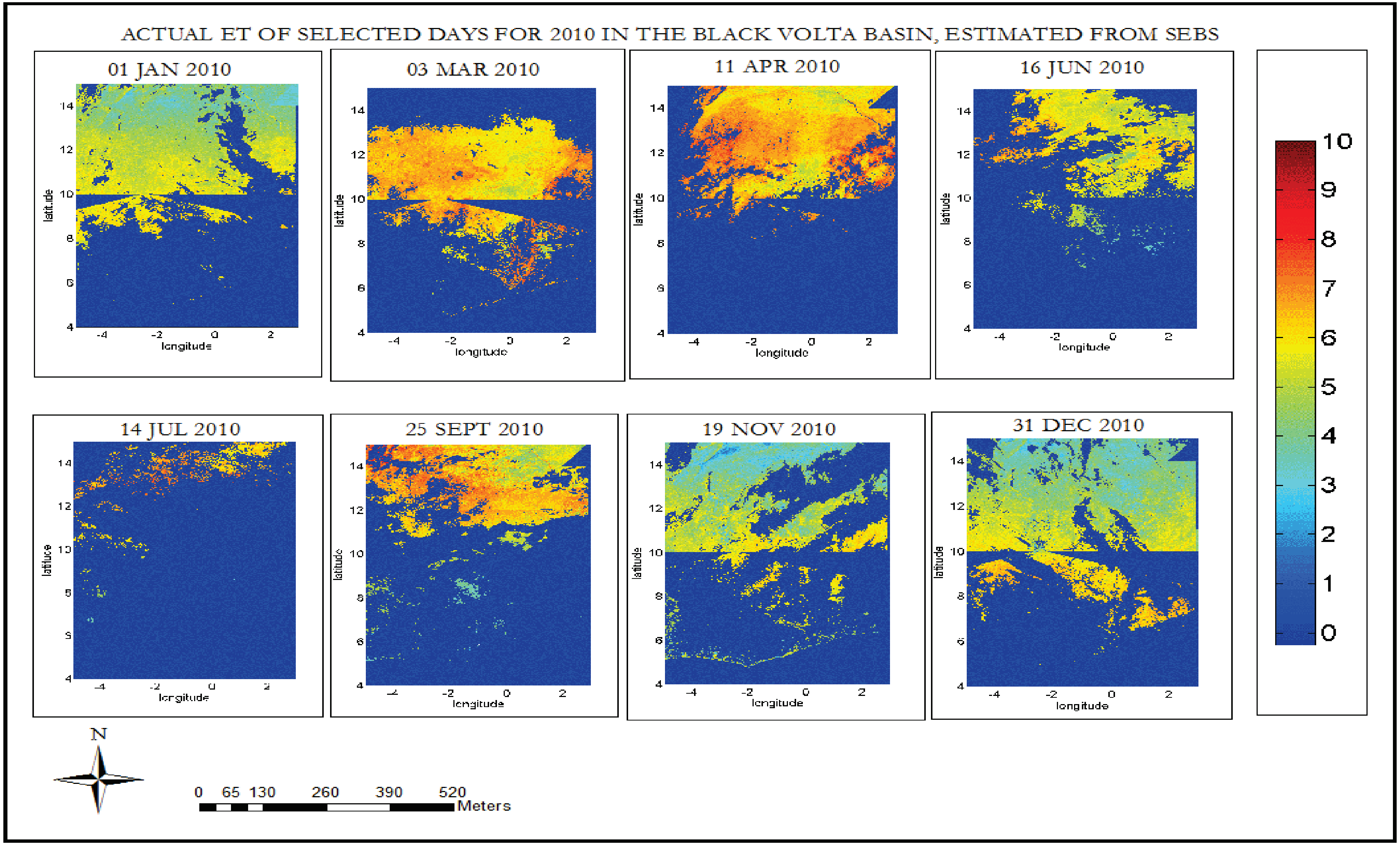

Figure 5:2 ETa map for selected days in the year 2010

5.1.1. ETa for stations in Black Volta Basin for January 2010

Daily maximum ETa in the month of January is 6.27mm. Mean ETa is 4.89mm with a standard deviation of 0.94mm. Wa has a daily maximum ETa in the month of January as 5.93mm. Mean ETa is 4.94 mm with a standard deviation of 0.47mm. Maximum daily ETa for Wenchi is 6.37mm and mean ETa value is 5.65 mm with a standard deviation of 0.70. Maximum daily ETa for Sunyani is 6.46mm and mean ETa for calculated days is 5.93 mm with a standard deviation of 0.41mm. Figure 5:3 show the ETa estimated for the four synoptic stations.

.

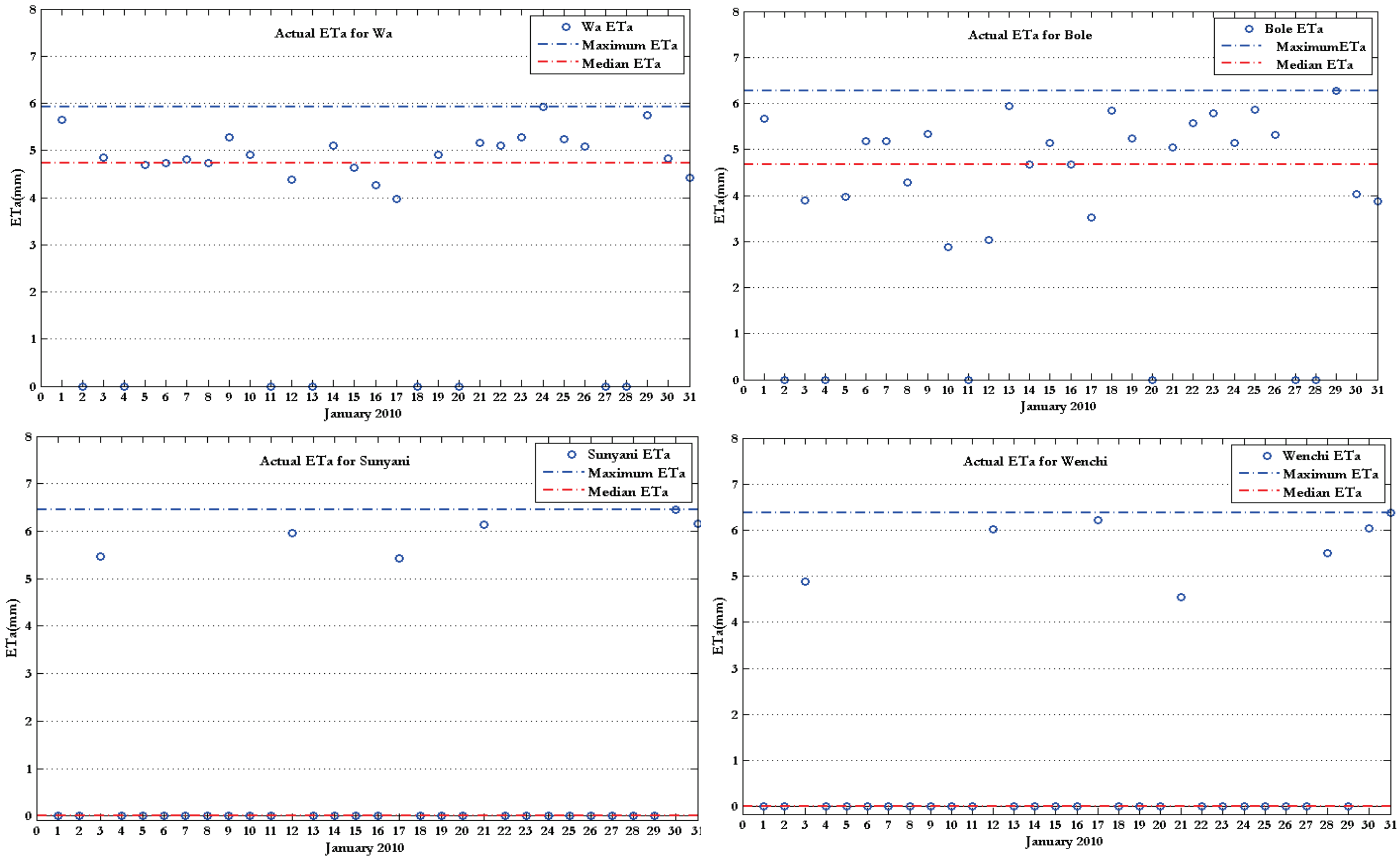

Figure 5:3. Actual ET for Stations in the Black Volta Basin for January 2010

5.2. Results from Monte Carlo Simulations.

With reference to this thesis these uncertainties are reported as daily uncertainties. The daily means, median and standard deviation are used to illustrate the output of the Monte Carlo uncertainty analysis for each individual synoptic station. 95th and 5th percentiles are used to show the maximum and minimum daily values.

5.2.1. Uncertainty analysis of Bole output

Monte Carlo simulation results of ETa for Bole in the Black Volta Basin are shown in Figure 5:4 . The output distribution for Bole was not normally distributed although a normal PDF was assumed for the identified source of input uncertainty. The median was greater than the mean and was negatively skewed (Figure 5:4)

Figure 5:5 , Figure 5:6 and Figure 5:7 describe the output distribution of stations Wa, Wenchi and Sunyani respectively.

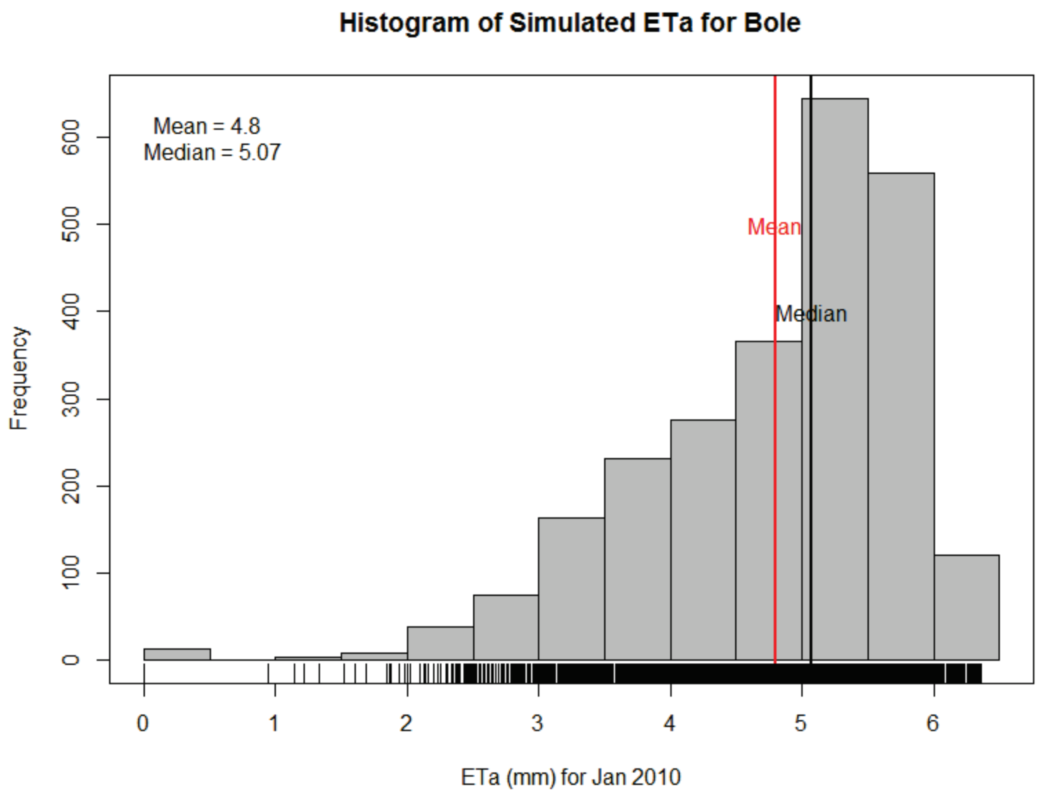

Figure 5:4 Representation of simulated actual ETa for Bole.

The mean and the median displayed in the histogram are the sample mean and median respectively. They describe the central point of the distribution.

Table 5:1 shows the mean, standard deviation and the end points of the distribution for Bole. The values are the daily values for estimated days for the month of January. The mean is the sample mean from 100 simulations per day. The output uncertainty in given as the standard deviation simulated output. The mean daily ETa per 100 simulations per day has a range of 2.96mm to 5.79mm per day. Minimum ETa per day is ~1.86 mm and maximum ETa is ~6.34 mm. Maximum and minimum are shown as the 5th and 95th percentiles in Table 5:1. Daily standard uncertainty characterized by the standard deviation ranges from 0.13mm to 1.38 mm per day.

Date	**Mean daily ETa(mm)**	**Standard Deviation(mm)**	**5th percentile(mm)**	**95th percentile (mm)**
1-Jan-10	5.64	0.13	5.45	5.79
3-Jan-10	3.92	0.40	3.27	4.61
5-Jan-10	3.83	0.79	3.11	4.56
6-Jan-10	5.17	0.22	4.79	5.48
7-Jan-10	5.12	0.17	4.84	5.35
8-Jan-10	4.18	0.80	3.46	4.80
9-Jan-10	5.25	0.48	4.96	5.58
10-Jan-10	2.96	0.60	1.86	3.72
12-Jan-10	3.02	0.52	2.14	4.12
13-Jan-10	5.79	0.84	5.70	6.06
14-Jan-10	4.63	0.28	4.17	5.11
15-Jan-10	5.08	0.56	4.72	5.41
16-Jan-10	4.70	0.24	4.36	5.15
17-Jan-10	3.45	0.53	2.43	4.21
18-Jan-10	5.79	0.59	5.68	6.03
19-Jan-10	5.25	0.22	4.88	5.58
21-Jan-10	5.06	0.29	4.56	5.48
22-Jan-10	5.55	0.18	5.27	5.85
23-Jan-10	5.79	0.19	5.44	6.09
24-Jan-10	5.09	0.36	4.51	5.61
25-Jan-10	5.87	0.12	5.69	6.03
26-Jan-10	5.30	0.22	4.95	5.66
29-Jan-10	5.63	1.38	2.99	6.34
30-Jan-10	4.05	0.36	3.48	4.70
31-Jan-10	3.85	0.48	2.99	4.57

Table 5:1 Summary for Bole January 2010 uncertainty evaluation

5.2.2. Uncertainty analysis of Wa output

ETa output distribution of uncertainty analysis for Wa is shown in Figure 5:5. The output distribution for Wa does not show a clearly skewed distribution. The mean was slightly greater than the median which is a positively skewed distribution.

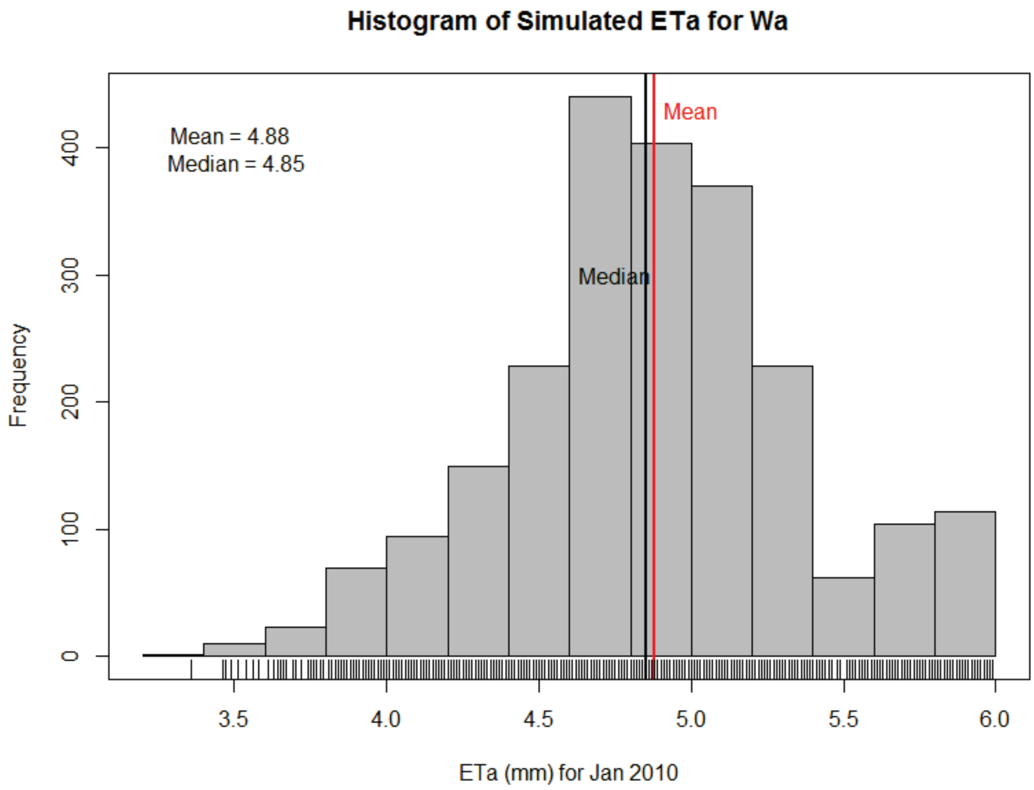

Figure 5:5 Representation of simulated actual ETa for Wa.

The mean daily ETa ranges from 4.28mm to 5.88mm with standard deviation from 0.11mm to 0.34mm. Minimum ETa per day is ~3.58mm and maximum ETa is ~5.97mm daily. Table 5:2 gives a summary of the output of the Monte Carlo uncertainty analysis for Wa.

Date	Mean daily ETa(mm)	Standard Deviation(mm)	5th percentile(mm)	95th percentile (mm)
1-Jan-10	5.39	0.34	4.72	5.66
3-Jan-10	4.81	0.15	4.57	5.08
5-Jan-10	4.67	0.15	4.44	4.88
6-Jan-10	4.65	0.22	4.35	4.83
7-Jan-10	4.68	0.21	4.25	4.85
8-Jan-10	4.62	0.24	4.18	4.85
9-Jan-10	5.15	0.17	4.82	5.31
10-Jan-10	4.76	0.27	4.16	5.00
12-Jan-10	4.39	0.20	4.09	4.71
14-Jan-10	5.08	0.14	4.82	5.25
15-Jan-10	4.55	0.26	4.13	4.82
16-Jan-10	4.28	0.17	3.95	4.47
17-Jan-10	3.96	0.22	3.58	4.31
19-Jan-10	4.87	0.12	4.68	5.07
21-Jan-10	5.16	0.14	4.93	5.38
22-Jan-10	5.11	0.13	4.89	5.33
23-Jan-10	5.27	0.11	5.07	5.45
24-Jan-10	5.88	0.14	5.54	5.97
25-Jan-10	5.03	0.34	4.11	5.38
26-Jan-10	4.99	0.23	4.72	5.17
29-Jan-10	5.73	0.11	5.56	5.91
30-Jan-10	4.82	0.15	4.55	5.06
31-Jan-10	4.39	0.24	4.07	4.86

Table 5:2 Summaries for Wa January 2010 uncertainty evaluation

5.2.3. Uncertainty analysis of Wenchi output

The distribution is negatively skewed. Mean daily ETa range is from 5.21mm to 6.37mm, standard deviation ranges from 0.15 mm and 1.31 mm. Maximum and minimum ETa is between ~6.25 mm and ~2.68 mm. Figure 5:6 and Table 5:3 summarize the output of the uncertainty analysis for Wenchi.

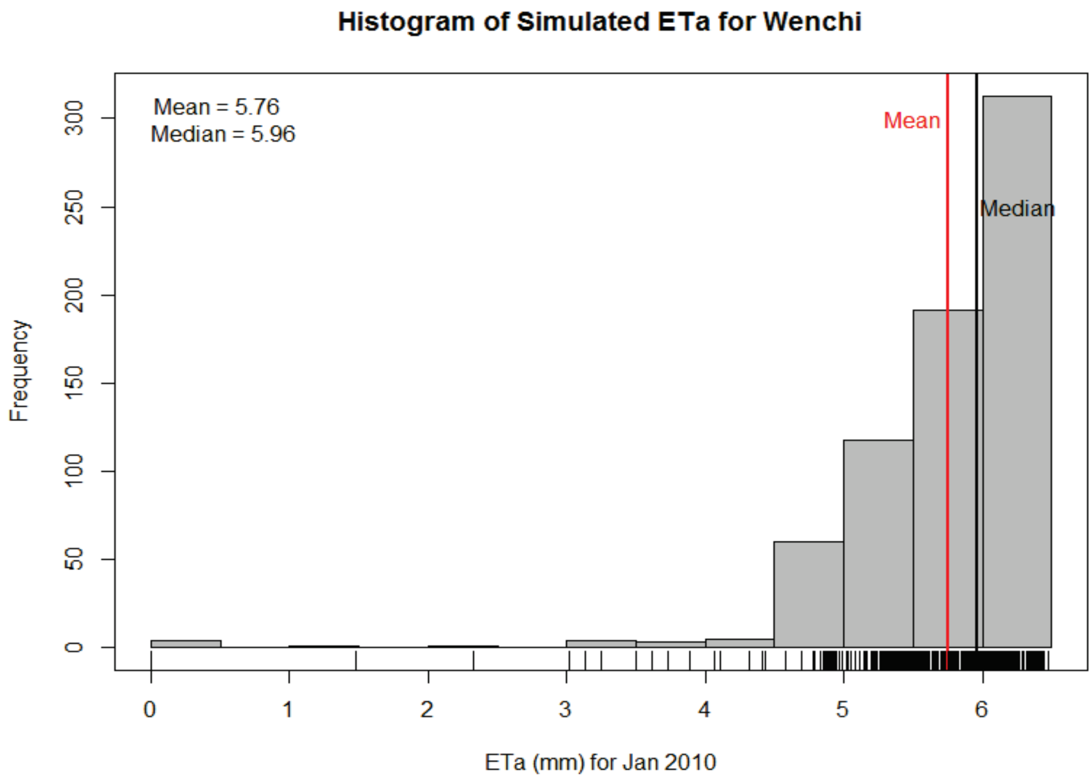

Figure 5:6 Representation of simulated actual ETa for Wenchi

Date	Mean daily ETa(mm)	Standard Deviation(mm)	5th percentile(mm)	95th percentile (mm)
3-Jan-10	5.28	0.44	4.86	5.93
12-Jan-10	5.99	0.15	5.70	6.23
17-Jan-10	6.01	0.33	5.33	6.25
21-Jan-10	5.21	1.31	2.68	6.23
28-Jan-10	5.44	0.56	5.36	5.64
30-Jan-10	5.99	0.16	5.76	6.18
31-Jan-10	6.37	0.04	6.32	6.42

Table 5:3 Summaries for Wenchi January 2010 uncertainty evaluation

5.2.4. Uncertainty analysis of Sunyani output

Mean daily ETa for Sunyani ranges from 5.38 mm to 6.44 mm, standard deviation range from 0.08 mm to 0.39 mm. Maximum and minimum ETa is ~6.51 mm to ~4.77 mm. The distribution is negatively skewed as median is greater than mean. Figure 5:7 and Table 5:4 summarize the output of the uncertainty analysis for Sunyani.

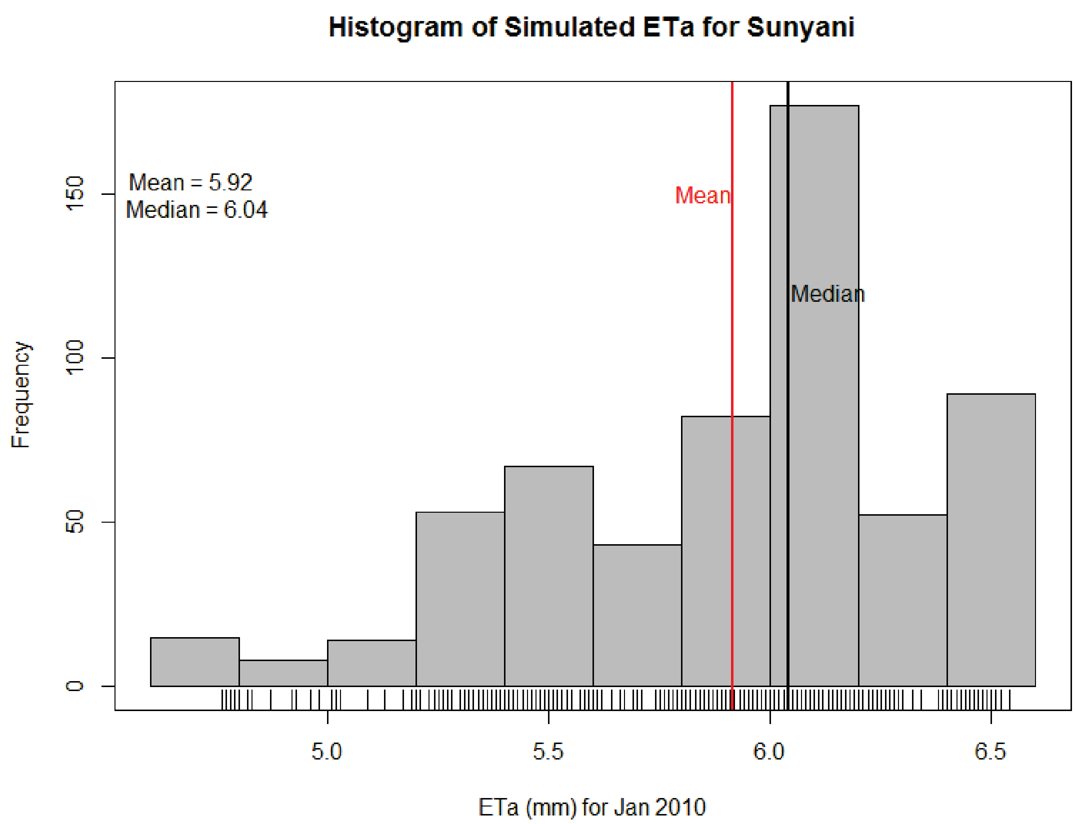

Figure 5:7 Representation of simulated actual ETa for Sunyani

Date	Mean daily ETa(mm)	Standard Deviation(mm)	5th percentile(mm)	95th percentile (mm)
3-Jan-10	5.38	0.39	4.77	5.82
12-Jan-10	5.97	0.1	5.83	6.18
17-Jan-10	5.43	0.09	5.29	5.57
21-Jan-10	6.12	0.08	5.98	6.25
30-Jan-10	6.44	0.09	6.39	6.51
31-Jan-10	6.15	0.09	6.02	6.26

Table 5:4 Summaries for Sunyani January 2010 uncertainty evaluation

5.3. Variability in simulated ETa estimates.

Boxplots are used in this section to show the distribution of the simulated ETa estimates and how much the estimates differ from each other in a day. The baseline ETa estimate is used as a check on the simulated daily mean ETa. Variability in the entire simulated ETa as well as standard error of the daily mean is analysed. Figure 5:8, Figure 5:9, Figure 5:10 and Figure 5:11 are used to illustrate the distributions.

Interquartile range estimated for Bole is from 0.13 mm and 0.89 mm per day. The standard error of the mean simulated ETa ranges from 0.01mm to 0.13 mm per day. Figure 5:8 show the spread of daily ETa values for Bole in the month of January 2010. It is expected that the variability about the mean will decrease as sample size increases. See Table 7:1 (Appendix D) for daily standard errors, confidence intervals and daily interquartile ranges for Bole.

5.3.1. Distribution of simulated ETa estimates for Bole

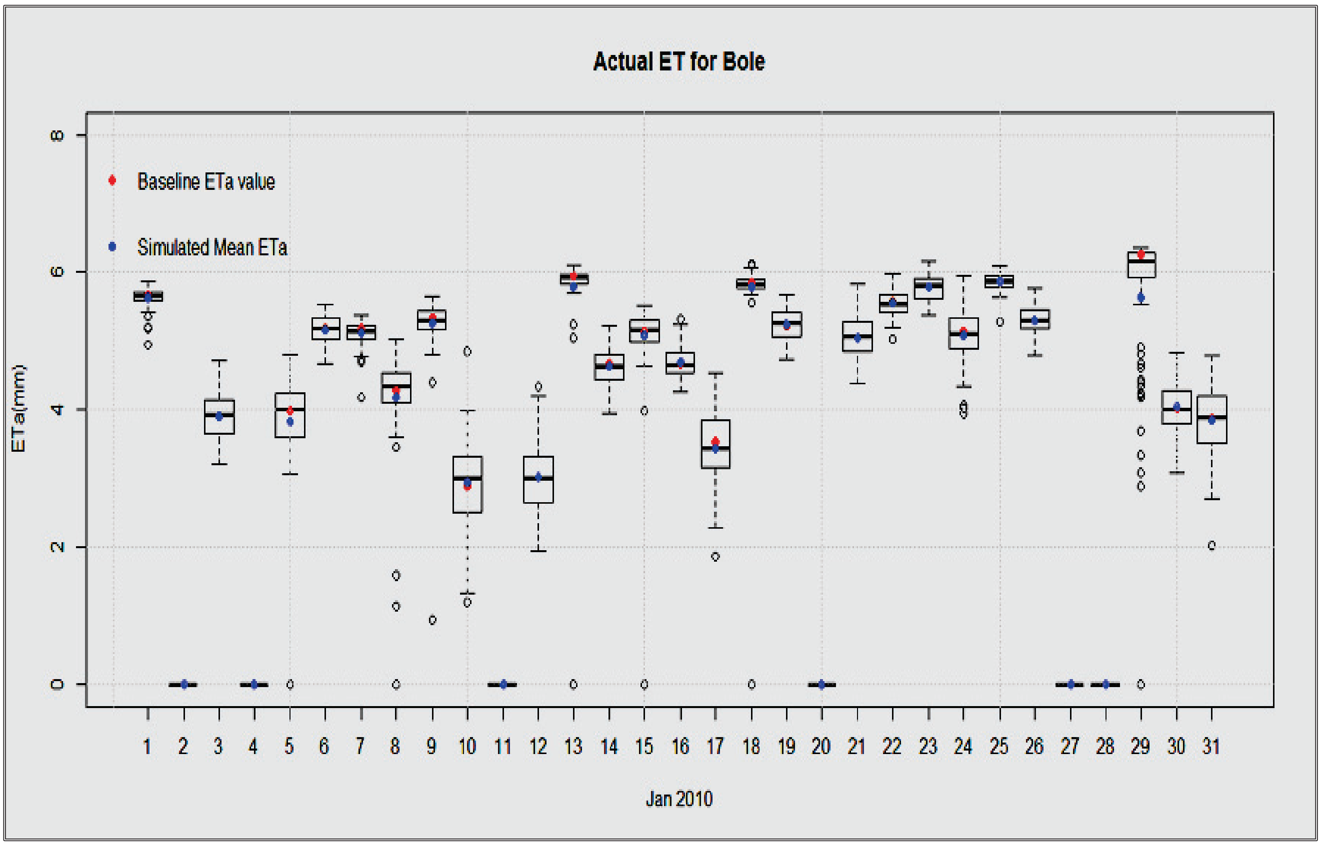

Figure 5:8 Boxplot showing the baseline ETa and simulated ETa of Bole for January 2010.

Baseline ETa values are shown in red dots.

5.3.2. Distribution of simulated ETa estimates for Wa

The interquartile range for Wa is from 0.04mm to 0.32mm per day. Standard error of the mean ranges from 0.01mm to 0.03mm. The results are shown graphically by Figure 5:9 and tabulated in Table 7:2 (Appendix D) for daily standard errors and confidence intervals for Wa.

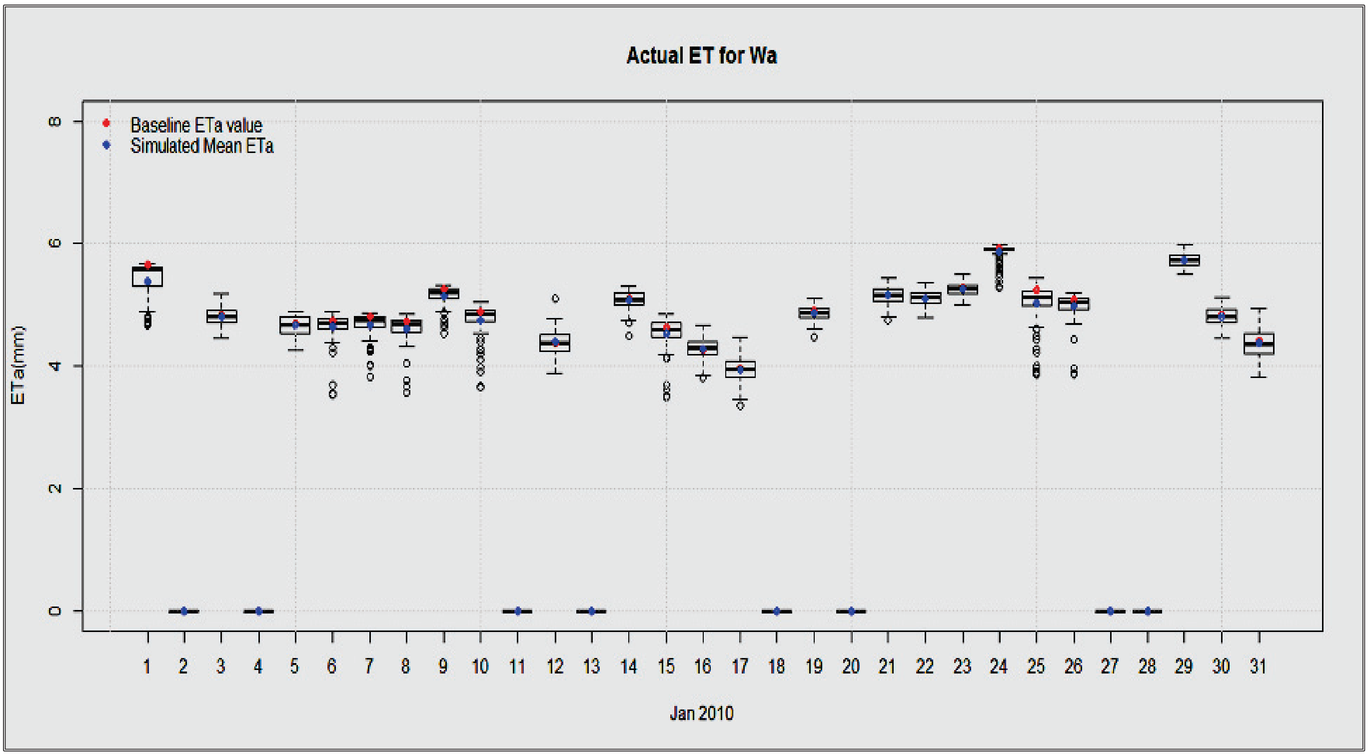

Figure 5:9 Boxplot showing baseline ETa and simulated ETa of Wa for January 2010.

5.3.3. Distribution of simulated ETa estimates for Wenchi

Result for Wenchi is illustrated in Figure 5:10. The daily interquartile range is from 0.04mm to 1.21mm. The standard error of the mean is ranges from 0.004mm to 0.13mm. See Table 7:3 (Appendix D) for fully estimated daily values.

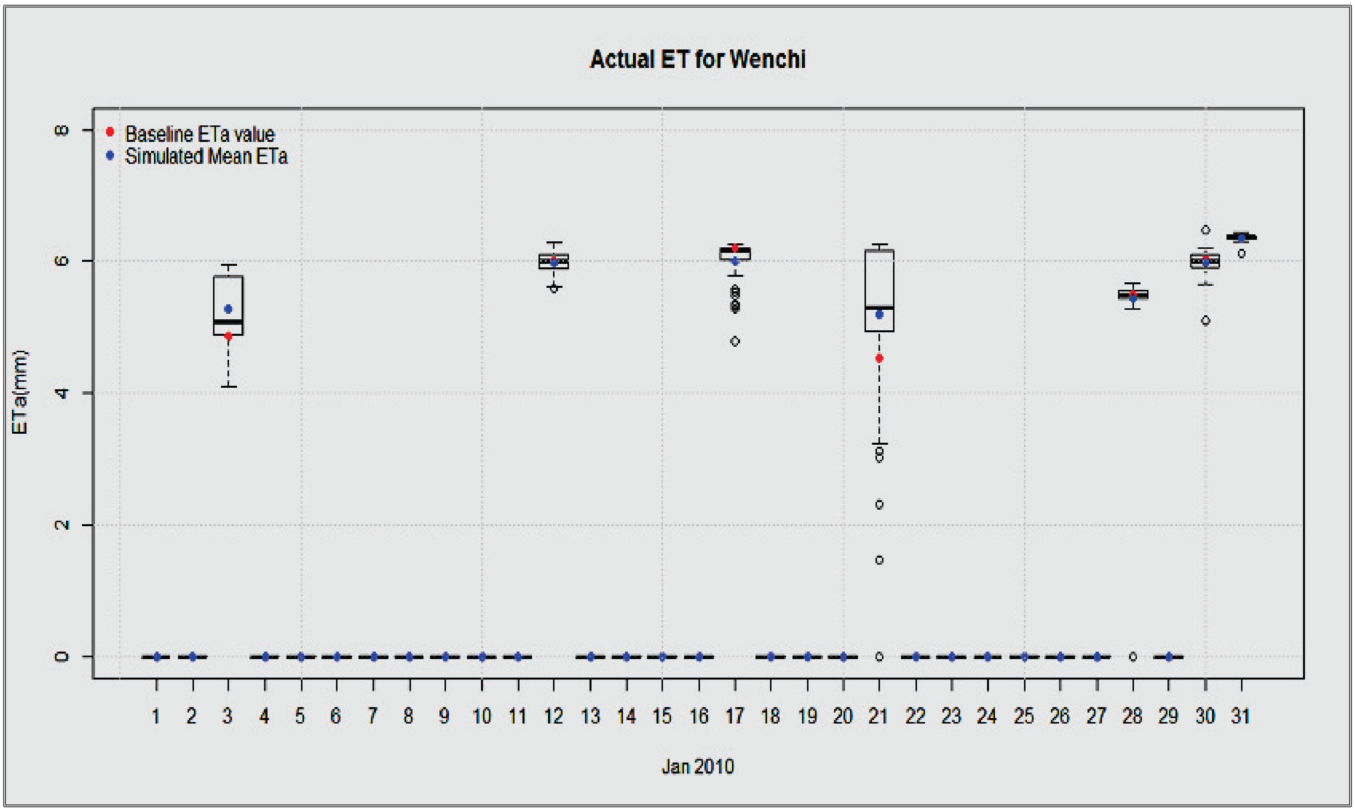

Figure 5:10 Boxplot showing the baseline ETa and simulated ETa of Wenchi for January 2010.

5.3.4. Distribution of simulated ETa estimates for Sunyani

The interquartile range is from 0.10mm to 0.75mm per day. The standard error of the mean is from 0.008mm to 0.04mm (see Figure 5:11 for graphical representation). See Table 7:4 (Appendix D) for daily standard errors and confidence intervals for Sunyani.

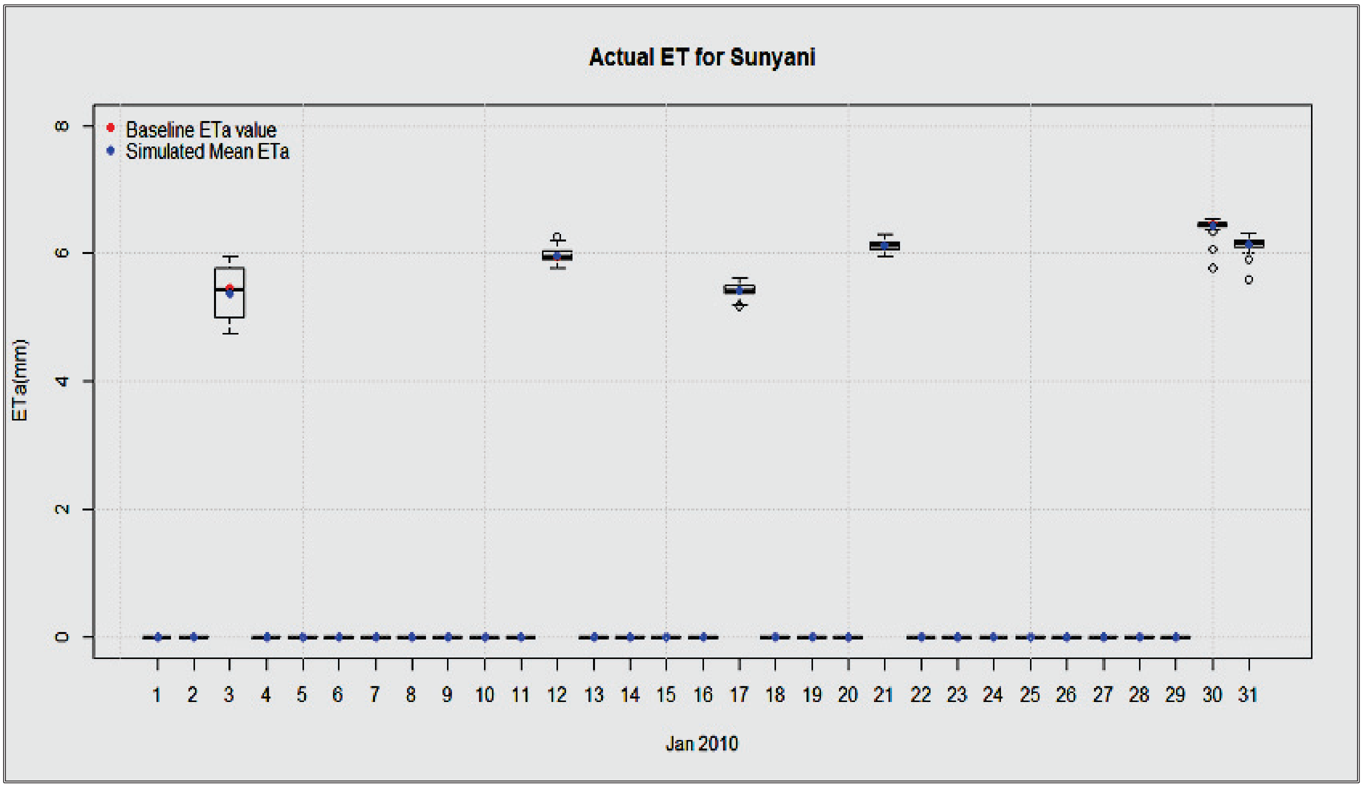

Figure 5:11 Boxplot showing the baseline ETa and simulated ETa of Sunyani for January 2010.

.

5.4. Difference in baseline output ETa and simulated output ETa

5.4.1. Mean error in outputs

Mean error (ME) is estimated per day to check for any bias in the estimates. It tells whether they over estimates or underestimate. A positive mean error shows over estimation and negative show under estimation. Figure 5:12 shows a mean error of -0.6mm to 0.08mm for Bole, -0.26mm to 0.006mm for Wa, -0.19mm to 0.67mm for Wenchi and -0.08mm to 0.013mm for Sunyani. Figure 7:3 (appendix E) is a histogram showing the distribution of errors across the four stations

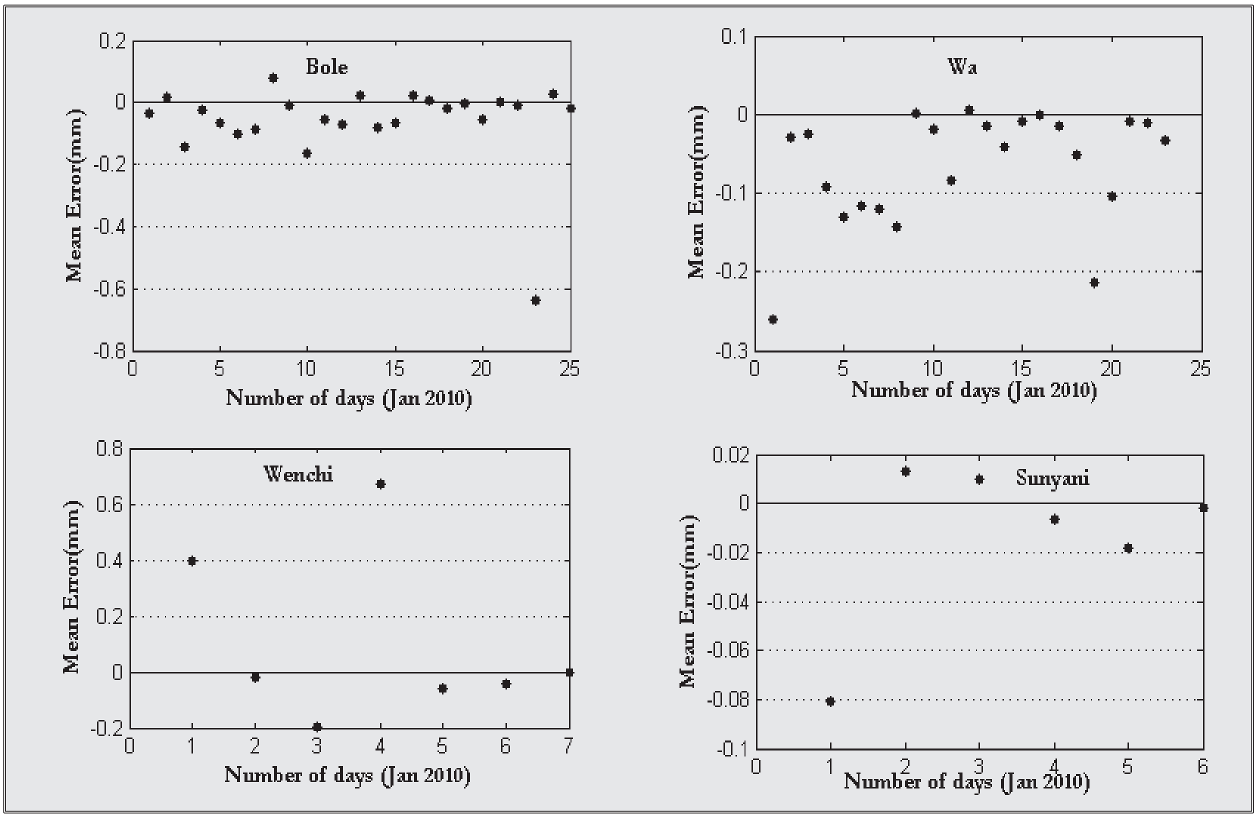

Figure 5:12 Mean Errors in ETa for Black Volta Basin

5.4.2. Root mean square error (RMSE)

The root mean square error (RMSE) tells how far on average the simulated ETa estimates are from the baseline ETa estimates. Figure 5:13 show the RMSE of individual stations. Bole has RMSE ranging from 0.11mm to 1.52mm per day and 0.45mm on average. Wa has RMSE ranging from 0.11mm to 0.43mm daily with 0.21mm on average. Sunyani with 0.08mm to 0.39mm daily has an average of 0.14mm and that of Wenchi ranges from 0.04mm to 1.47mm daily with an average of 0.48mm.

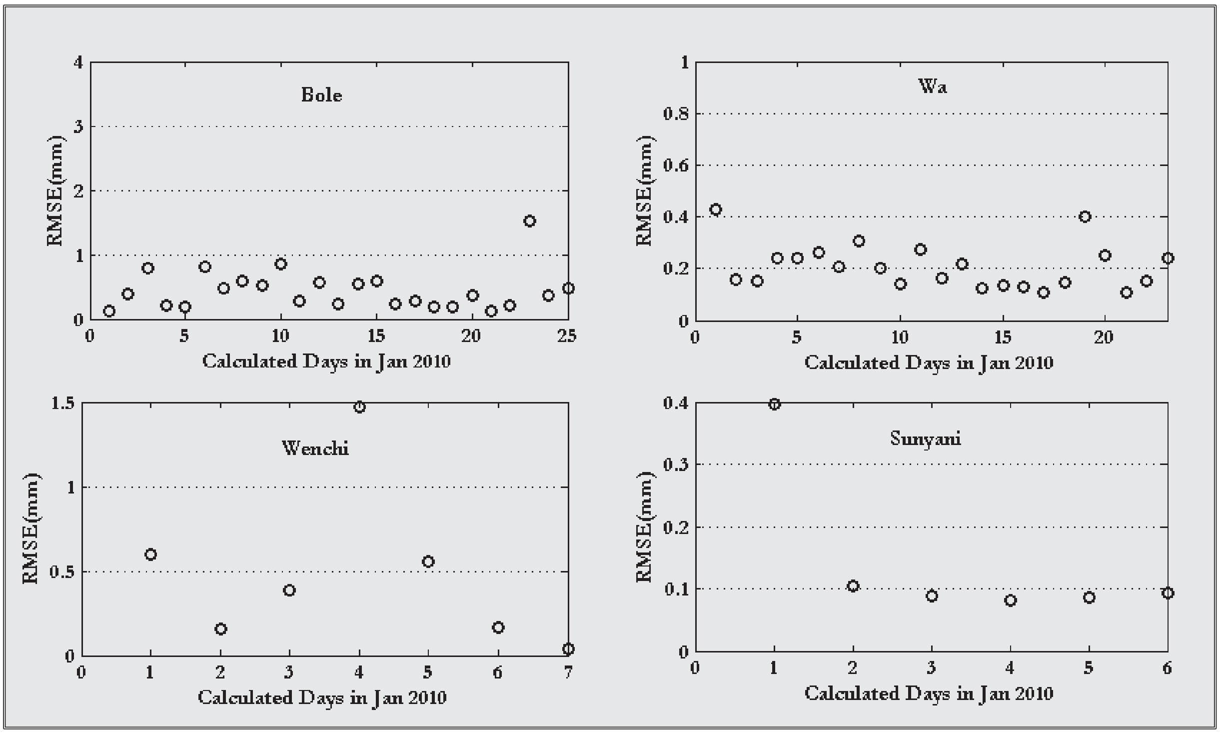

Figure 5:13 RMSE plots for days with calculated ETa

5.5. Comparison between wet and dry regions of study area.

Dry areas i.e. Bole and Wa have daily baseline ETa ranging from 2.88mm to 6.27mm and daily mean simulated ETa as 2.95mm to5.88. Baseline ETa for wet areas i.e. Wenchi and Sunyani ranges from 4.54mm to 6.46mm while mean simulated ETa is from 5.21mm to 6.44mm. Figure 5:14 shows the graphical representation of these areas and their uncertainty.

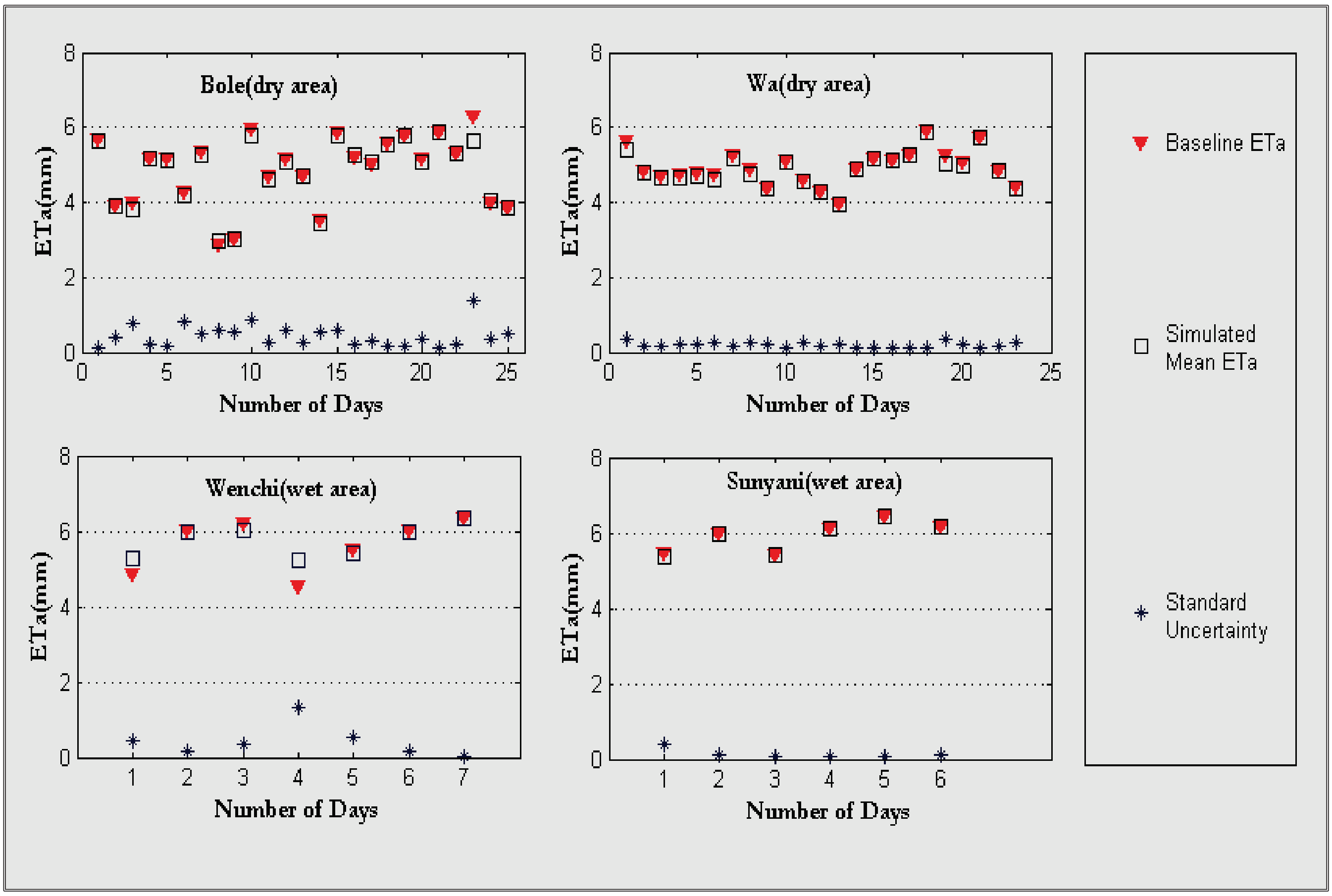

Figure 5:14 comparing wet and dry regions of the study area.

5.6. Comparing Actual ET and Potential ET of Meteorological stations in study Area

This comparison is done as both methods are estimating on the same reference surface. Figure 5:15 shows the comparison for the various stations in the Black Volta Basin.

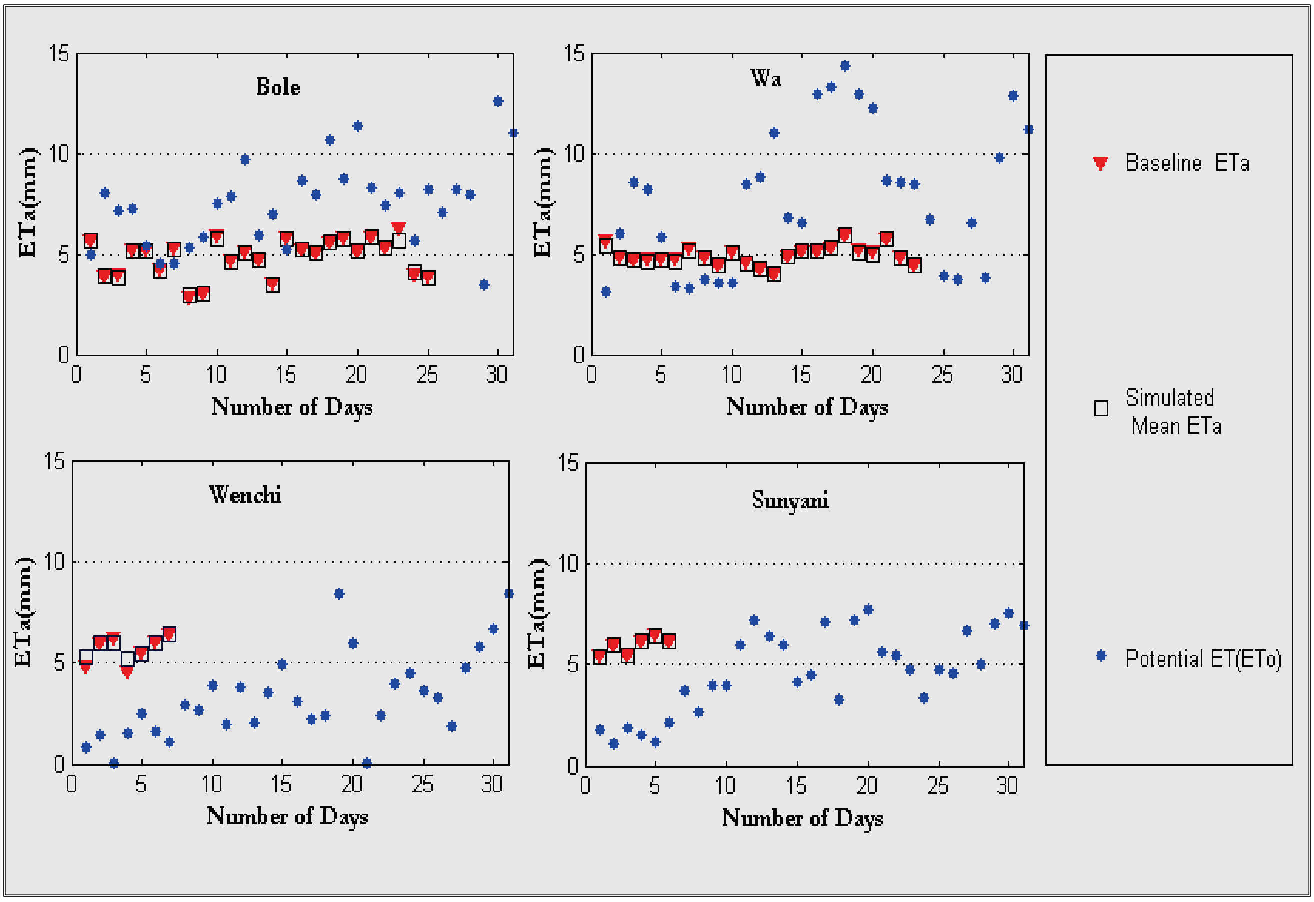

Figure 5:15 Comparison between Potential ET and Actual ET

5.7. Summary

Individual errors are used to show the differences in the simulated outputs and baseline values. The mean of these errors show whether a particular set of measurements are underestimated (negative value) or overestimated (positive values). The RMSE in this contest is used to show how biased the simulated values and comparison to baseline values. The baseline values are only assumed to be the true observations since the actual true value is unknown. The baseline ETa values are the only real representation since its estimates from the observed measurements of from the selected stations.

Standard uncertainty from Monte Carlo simulation is given as the standard deviation. Mean and median of distributions are given to measure of central tendencies.

6. DISCUSSION

Uncertainty in different aspects of input data to SEBS have been described in various articles and publications such as J. Timmermans et al. (2011), Van der Kwast et al. (2009), Gibson et al. (2011) etc. The estimation of ET is a complicated process which requires different input data and execution steps. It is therefore inevitable that there are sources of uncertainty from input data, spatial heterogeneity of study, resolution of input data, processing errors etc. (Gibson et al., 2010). Sensitivity to determine the aspects of the input data that mostly influence the output has been discussed by various authors and book writers e.g. Van der Kwast et al. (2009), Tol and Parodi (2012), Su (2002) etc.

In this study uncertainties associated with input in situ meteorological data in ET estimates using the SEBS algorithm is analysed. Sources of uncertainty focused on are in situ meteorological variables which are temperature; sunshine hours and wind speed (see Table 4:1). Results indicate that due to measurement uncertainties in these meteorological variables as stated in WMO-No.8 (2008), individual stations studied in the Black Volta Basin of Ghana have standard uncertainty ranging from 0.11mm to 1.38mm on daily basis stated as the standard deviation after running Monte Carlo simulation for the SEBS algorithm using sources of uncertainty as in situ meteorological variables. See Table 5:1, Table 5:2, Table 5:3, and Table 5:4 for summary on individual stations.

A study conducted by Opoku-Duah et al. (2008) in the Savannah (dry or dessert) area of the Volta Basin estimated regional uncertainty in ET to be around 0.37mm using MODIS, 0.86mm using AATSR and 0.42mm using Landsat ETM+. This goes to stress the fact that there are inherent uncertainty in the estimating of ET over Black Volta although Opoku-Duah et al. (2008) did not explicitly indicate which input data as a source of uncertainty.

The dry parts of this study area (Bole and Wa) which is comparable to the local study area (Tamale) of Opoku-Duah et al. (2008) in terms of their geographical location and atmospheric conditions has standard deviation ranging from 0.13mm to 1.38mm and 0.11mm to 0.34mm respectively (see Table 5:1 and Table 5:2). In his study (Opoku-Duah et al., 2008) estimated the standard deviation of Tamale to be approximately 0.66mm. Other stations in this study, Wenchi and Sunyani have daily standard deviation ranging from 0.15mm to 1.31mm and 0.08mm to 0.39mm.

SEBS uses two sources of temperature which are land surface temperature and air temperature. In the determination of net radiation and ground heat flux, the use of land surface temperature plays an important role in sensible heat flux which intern influences the output ET. Air temperature which is considered in this study directly affects the evaporative process, uncertainties in air temperature measurements can lead to inaccurate ET thereby introducing uncertainty in the output (Gibson et al., 2011).

Wind speed measurements are dependent on the reference height at which it is measured particularly in the implementation of SEBS model in tall canopy areas. The combination of the reference height at which wind speed is measured and displacement height aid the process of determining sensible heat flux, therefore the uncertainty introduced when the displacement height get closer to the wind speed must be addressed as it influences the final ET. The aerodynamic resistance becomes low when there is higher wind speed (Gibson et al., 2011). ETa estimates for SEBS will therefore be high in areas where the wind speed is high.

Although this thesis is focused on the uncertainties relating to in situ meteorological variables, other sources of uncertainties such as parameterization, model structure etc. is inherent. Some previous studies have found out that land surface temperature can have noticeable effect in the estimation of sensible heat thereby affecting the output ET. Example Su (2002) estimated RMSE of sensible heat to be in the region of 21.22 Wm^{-2} when input variable are within 50% of their actual value. Tol and Parodi (2012) noted that in order to come up with reasonable ET output, the temperature gradient should be better than 2°C.

In this study, estimated mean errors between the simulated ETa and baseline ETa are shown graphically in Figure 5:12. The results show that the simulation underestimates the baseline ETa by a range of -0.01mm to -0.64mm in some days and overestimates by 0.01mm to 0.67mm for other days across all stations in the region. There are more days of underestimation than overestimation. Table 7:5 (appendix E) gives details of individual stations and their daily ME estimates. On average, RMSE estimates show that the simulated ETa values are a range of 0.13mm to 1.52mm away from baseline ETa across all stations on daily basis. See Table 7:6 (appendix E) for detailed daily values.

The results further appear to show significant variability in the mean simulated ETa estimates. Interquartile estimates show a range of 0.04mm to 1.21mm daily while standard error of the mean ranges from 0.004mm to 0.13mm daily across the four stations. The variability is more significant and high in the dry areas i.e. Bole and Wa. See Table 7:1, Table 7:2, Table 7:3, Table 7:4 for details of individual station and their 95% confident limit. The graph in Figure 4:1 appears to shows variation in the in situ variables temperature, sunshine hours and wind speed across the month of January. Measurement conditions may not be the same each day as such variability is expected in output variable. There's however a large variability in individual daily values of wind speed and air temperature in all stations. Air temperature and wind speed may have lower spatial variability as a result of atmospheric disturbances (Ershadi et al., 2013).

In the analysis of this study, wet areas of the study region (Sunyani and Wenchi) are compared to dry areas (Bole and Wa). Baseline ETa for wet areas ranges from 4.54mm to 6.46mm and that of dry areas is 2.88mm to 6.27mm. Simulated daily mean ETa for wet areas ranges from 5.21mm to 6.44mm and that of dry areas is from 2.95mm to 5.88mm. Sensible heat which is major component of SEBS and the outcome of ETa takes the minimum value under wet limits where the evaporation is subject to the available energy with reference to the surface under study and its atmospheric conditions. The actual sensible heat is restricted in a range by sensible at wet limit. At dry limit the sensible flux is dependent on available energy (Su, 2002). Dry areas of the study especially Bole have standard deviation ranging from 0.12mm to 1.38mm while Sunyani have uncertainty ranging from 0.08mm to 0.39mm.

In comparing potential and actual ET there is one noticeable effect which is the fact that potential ET is calculated for days whiles SEBS is dependent on the availability of satellite and less cloud cover. In the calculation of potential ET it is assumed that the water needed for evapotranspiration is not limited to any factor. Comparing actual and potential evapotranspiration may not be the correct way. Penman Montieth estimates assumes adequate water availability for estimation of ET from the reference surface (Allen, 2000). SEBS calculates according to the actual conditions of the area.

7. CONCLUSIONS AND RECOMMENDATIONS

7.1. Conclusions

The objective of this thesis was to analyse the uncertainty SEBS based ET estimates given a range of input uncertainty from in situ meteorological data in the area of the Black Volta basin of Ghana. The difference in ETa values in the wet and dry areas of the study region were compared to see how SEBS estimates and the related uncertainties differ in these areas.

Emphasis was placed on the uncertainty in input data realised from four meteorological stations situated in these areas namely Bole, Wa Sunyani airport and Wenchi. Below are some of the conclusions from this thesis. Uncertainty analysis was done using the stated required uncertainties from the (WMO-No.8, 2008).

The results show that there are inherent uncertainties in SEBS based ET estimates given a range of input meteorological uncertainty with their probability distribution functions. The use Monte Carlo based simulation for uncertainty analysis allows for full range of coverage input probability distribution function. The result shows that SEBS ETa estimates for this area at 95% confidence interval may be within a range of 2.84mm to 5.95mm for Bole, 3.91mm to 5.91mm for Wa, 4.96mm to 6.38mm for Wenchi and 5.30mm to 6.46mm for Sunyani.

The level of uncertainty estimated and discussed in the previous chapter is as result of introduced uncertainty in input meteorological data; however it might differ at certain scenario when conditions and set of input data considered being sources of uncertainty changes. The results demonstrate Surface Energy Balance System (SEBS) can be used to estimate actual evapotranspiration and turbulent heat fluxes. It can also take care of spatial and temporal ETa estimations from large scale to point estimates with a certain level of uncertainty which is dependent on the introduced input data uncertainty.

7.2. Recommendations

1. The analysis of uncertainties for three meteorological input variables to SEBS was analysed together and the effect on the output quantity assessed. Information about how each parameter affect the output parameter is given as their effect is characterized together. I therefore recommend for further analysis of uncertainty on the individual measurements given their probability distribution functions. Varying each of them one at a time and holding the others constant can highlight the individual effects. It will also enable us to ascertain which meteorological variable introduces most uncertainty to the output ET value. Preferably I would recommend a variance-based sensitivity analysis, a method also used by Hamm et al. (2006). It will allow for model-independent and global based sensitivity analysis.

2. SEBS uses various sets of data, including satellite data that also come with their own levels of uncertainties. I therefore recommend that the uncertainties of the satellite measurements should be looked into to better understand the nature of uncertainties in the SEBS estimates and how each set of data may affect the output and to what extent. Several studies including Tol and Parodi (2012) , (W. J. Timmermans et al., 2007) etc. have identified land surface temperature and sensible heat flux as having high sensitivity to SEBS. Running

3. I would also recommend for a further number of Monte Carlo simulation of the model input data to fully ascertain the level and range of uncertainty in the input data. (see Table 7:7)

7.3. Limitations

1. Data was not readily available; example mean daily temperature had to be estimated from maximum and minimum temperature of the day. From (Su, 2002) he explained that SEBS used instantaneous remote sensing data while the in-situ data used together with the remotely sensed data are not instantaneous. This may well affect the result.

2. Monte Carlo limitation has its own limitations; runtime of model simulation can be long when complex models are involved. Also the selecting the appropriate probability distribution function for input parameters can be an intricate task as result of lack of information or understanding about the nature of the variables under study (Ángeles Herrador & González, 2004).

LIST OF REFERENCE

Allen, R. G. (2000). Using the FAO-56 dual crop coefficient method over an irrigated region as part of an evapotranspiration intercomparison study. Journal of Hydrology, 229(1–2), 27-41.

Allen, R. G., Pereira, L. S., Howell, T. A., & E.Jensen, M. (2011). Evapotranspiration information reporting: I. Factors governing measurement accuracy. Agricultural Water Management, 98(6), 899-920.

Allen, R. G., Pereira, L. S., Raes, D., & Smith, M. (1998). Crop evapotranspiration-Guidelines for computing crop water requirements-FAO Irrigation and drainage paper 56. FAO, Rome, 300, 6541.

Ángeles Herrador, M., & González, A. G. (2004). Evaluation of measurement uncertainty in analytical assays by means of Monte-Carlo simulation. Talanta, 64(2), 415-422.

Bastiaanssen, W. G. M. (1995). Regionalization of surface flux densities and moisture indicators in composite terrain, a remote sensing approach under clear skies in Mediterranean climates. Report 109, Agricultural Department, Wageningen, Netherlands.

Bastiaanssen, W. G. M., Menenti, M., Feddes, R., & Holtslag, A. (1998). A remote Surface energy balance algorithm for land (SEBAL). 1. Formulation. Journal of Hydrology, 212/213, 198-212.

BIPM, IEC, IFCC, ILAC, ISO, & IUPAC. (2008). IUPAP and OIML,"Evaluation of Measurement Data–Supplement 1 to the 'Guide to the Expression of Uncertainty in Measurement'–Propagation of distributions using a Monte Carlo method". Joint Committee for Guides in Metrology, JCGM, 101.

Brutsaert, W., & Sugita, M. (1992). Application of self-preservation in diurnal evolution of the surface energy budget to determine daily evaporation. J. Geophysical Res ,, 97, 18377-18382.

Cai, J., Liu, Y., Lei, T., & Pereira, L. S. (2007). Estimating reference evapotranspiration with the FAO Penman–Monteith equation using daily weather forecast messages. Agricultural and Forest Meteorology, 145(1–2), 22-35. doi: 10.1016/j.agrformet.2007.04.012

Decker, J. E., Eves, B. J., Pekelsky, J. R., & Douglas, R. J. (2011). Evaluation of uncertainty in grating pitch measurement by optical diffraction using Monte Carlo methods. Measurement Science and Technology, 22(2), 027001.

Elhag, M., Psilovikos, A., Manakos, I., & Perakis, K. (2011). Application of the SEBS Water Balance Model in Estimating Daily Evapotranspiration and Evaporative Fraction from Remote Sensing Data over the Nile Delta. Water Resources Management, 25(11), 2731-2742.

Ershadi, A., McCabe, M., Evans, J., Mariethoz, G., & Kavetski, D. (2013). A Bayesian analysis of sensible heat flux estimation: Quantifying uncertainty in meteorological forcing to improve model prediction. Water Resources Research, n/a-n/a. doi: 10.1002/wrcr.20231

Gibson, L. A., M¨unch, Z., Engelbrecht, J., & Conrad, J. E. (2010). Uncertainties in using remote sensing for water use determination: a case study in a heterogeneous study area in South Africa. Hydrology Earth System Science, 7, 6581–6612.

Gibson, L. A., Münch, Z., & Engelbrecht, J. (2011). Particular uncertainties encountered in using a pre-packaged SEBS model to derive evapotranspiration in a heterogeneous study area in South Africa. Hydrology and Earth System Sciences, 15(1), 295-310.

Gyau-Boakye, P., & Tumbulto, J. (2000). The Volta Lake and declining rainfall and streamflows in the Volta River Basin. Environment, Development and Sustainability, 2(1), 1-11.

Hamm, N. A. S., Hall, J. W., & Anderson, M. G. (2006). Variance-based sensitivity analysis of the probability of hydrologically induced slope instability. Computers & Geosciences, 32(6), 803-817.

Horne, K., Ban, H., Fielding, R., & Kennedy, R. (2012). Monte Carlo uncertainty estimation for an oscillating-vessel viscosity measurement. Metrologia, 49(4), 577.

Idso, S. B., Schmugge, T. J., Jackson, R. D., & Reginato, R. J. (1975). The utility of surface temperature measurements for the remote sensing of surface soil water status. Journal of Geophysical Research 80(C21).

JCGM:101. (2008). Evaluation of measurement data - Supplement 1 to the "Guide to the expression of uncertainty in measurement" – Propagation of distributions using a Monte Carlo method. Joint Committee for Guides in Metrology; 2008.

Jia, L., Su, Z., van den Hurk, B., Menenti, M., Moene, A., De Bruin, H. A. R., . . . Cuesta, A. (2003). Estimation of sensible heat flux using the Surface Energy Balance System (SEBS) and ATSR

measurements. Physics and Chemistry of the Earth, Parts A/B/C, 28(1–3), 75-88. doi: http://dx.doi.org/1
Kustas, W. P., & Daughtry, C. S. T. (1989). Estimation of the soil heat flux/net radiation ratio from spectral data. Agr. Forest. Meteorol.,, 49, 205–223.
Li, X. (2001). Estimation of Urumqi River Basin Evaporation with Remote Sensing. M.Sc. Thesis in Hydrological Engineering, UNESCO-IHE, Delft.
Linacre, E. (1992). Climate Data and Resources – A Reference and Guide. Routledge, London,, 366pp.
Marx, A., Kunstmann, H., Schüttemeyer, D., & Moene, A. F. (2008). Uncertainty analysis for satellite derived sensible heat fluxes and scintillometer measurements over Savannah environment and comparison to mesoscale meteorological simulation results. Agricultural and Forest Meteorology, 148(4), 656-667.
McCabe, M. F., & Wood, E. F. (2006). Scale influences on the remote estimation of evapotranspiration using multiple satellite sensors. Remote Sensing of Environment, 105(4), 271-285.
Melesse, A. M., W, A., & T, D. (2009). Evaporation Estimation of Rift Valley Lakes: Comparison of Models. Sensors, 9(12), 9603-9615.
Menenti, M. (1984). Physical aspects and determination of evaporation in deserts applying remote sensing techniques. Report 10, Inst. Land Water Managm. Res. (IWC). Wageningen, Niederlande; 202 Seiten, 117 Abb., 8 Farbilder, 55 Tab., 45, – DFL.
Monteith, J. L. (1973). Principles of Environmental Physics. Edward Arnold, London,. 241 PP.
Oguntunde, P. G. (2004). Evapotranspiration and complimentarity relations in the water balance of the Volta Basin : field measurements and GIS-based regional estimates. (Tevens proefschrift Bonn, 2004), Cuvillier, Göttingen. Retrieved from http://edepot.wur.nl/187640
Opoku-Duah, S. (2007). Remote sensing of energy and water fluxes over Volta Savannah catchments in West Africa. Durham University.
Opoku-Duah, S., Donoghue, D., & Burt, T. (2008). Intercomparison of Evapotranspiration Over the Savannah Volta Basin in West Africa Using Remote Sensing Data. Sensors, 8(4), 2736-2761.
Opoku-Duah, S., Kankam-Yeboah, K., Calabresi, G., & Lichtenegger, J. (1999). Retrieval of Landuse and Hydrology-based Parameters from Remote Sensing Satellite Synthetic Aperture Radar Data: The Case of the Volta Lake Basin in Ghana. Journal of Applied Science and Technology (JAST), Vol. 4(Nos. 1 & 2), pp. 44–58.
Paturel, J. E., Servat, E., & Delattre, M. O. (1997). Analysis of long-term rainfall series in West Africa and Central Non Sahelian in a context of climate variability. ORSTOM, Programme FRIEND AOC, 06 BP1203 Cidex1, Abidjan 06, Côte d'Ivoire. E-mail: eric.servat@mpl.orstom.fr.
Prince, S. D., Kerr, Y. H., Goutorbe, J.-P., Lebel, T., Tinga, A., Bessemoulin, P., . . . Gash, J. H. (1995). Geographical, biological and remote sensing aspects of the Hydrologic Atmospheric Pilot Experiment in the Sahel (HAPEX-Sahel). Remote Sensing of Environment, 51(1), 215-234.
Rauwerda, J., Roerink, G. J., & Su, Z. (2002). Estimation of evaporative fractions by the use of vegetation and soil component temperatures determined by means of dual-looking remote sensing. Wageningen: Alterra, Green World Research.
Shukla, J., & Mintz, Y. (1982). Influence of Land-Surface Evapotranspiration on the Earth's Climate Author(s) Source: Science, New Series. American Association for the Advancement of Science Stable, 215(4539), 1498-1501.
Su, Z. (2001). A Surface Energy Balance System (SEBS) for estimation of turbulent heat fluxes from point to continental scale. In: Advanced Earth Observation – Land Surface Climate, Z. Su and Jacobs, C. (Eds.). Publications of the National Remote Sensing Board (BCRS), USP-2, 01-02. 184pp.
Su, Z. (2002). The Surface Energy Balance System (SEBS) for estimation of turbulent heat fluxes. Hydrology. Earth System. Science, 6, 85 -100.
Su, Z. (2006). Estimation of the surface energy balance. Encyclopedia of hydrological sciences.
Su, Z., Li, X., Zhou, Y., Wan, L., Wen, J., & Sintonen, K. (2003a, 21-25 July 2003). Estimating areal evaporation from remote sensing. Paper presented at the Geoscience and Remote Sensing Symposium, 2003. IGARSS '03. Proceedings. 2003 IEEE International.
Su, Z., Yacob, A., Wen, J., Roerink, G. J., He, Y., Gao, B., . . . Diepen, C. A. v. (2003b). Assessing relative soil moisture with remote sensing data: theory, experimental validation, and application to drought monitoring over the North China Plain. Physics and Chemistry of the Earth, 28, 89-101.

Timmermans, J., van der Tol, C., Verhoef, A., Verhoef, W., Su, Z., van Helvoirt, M., & Wang, L. (2011). Quantifying the uncertainty in estimates of surface-atmosphere fluxes through joint evaluation of the SEBS and SCOPE models. Hydrol. Earth Syst. Sci. Discuss, 8, 2861-2893.

Timmermans, W. J., Kustas, W. P., Anderson, M. C., & French, A. N. (2007). An intercomparison of the surface energy balance algorithm for land (SEBAL) and the two-source energy balance (TSEB) modeling schemes. Remote Sensing of Environment, 108(4), 369-384.

Tol, C. v. d., & Parodi, G. N. (2012). Guidelines for Remote Sensing of Evapotranspiration, Evapotranspiration - Remote Sensing and Modeling. Dr. Ayse Irmak (Ed.), ISBN: 978-953-307-808-3, InTech, Available from: http://www.intechopen.com/books/evapotranspiration-remote-sensing-andmodeling/ Guidelines-for-remote-sensing-of-evapotranspiration.

Van der Kwast, J., Timmermans, W., Gieske, A., Su, Z., Olioso, A., Jia, L., . . . De Jong, S. (2009). Evaluation of the Surface Energy Balance System (SEBS) applied to ASTER imagery with flux-measurements at the SPARC 2004 site (Barrax, Spain). Hydrology and Earth System Sciences Discussion, 6(1), 1165-1196.

Wang, L., Parodi, G. N., & Su, Z. (2008). SEBS Module BEAM: A practical tool for surface energy balance estimates from remote sensing data. International Institute for Geo-Information Science and Earth Observation – ITC. WRS. P.O.Box 6, 7500 AA Enschede, The Netherlands, Email: lichun@itc.nl.

Washington, R., Harrison, M., Conway, D., Black, E., Challinor, A., Grimes, D., . . . G.; Todd, M. (2000). African climate change: Taking the shorter route. BAMS, 10, 1355-1365.

WMO-No.8. (2008). Guide to Meteorological Instruments and Methods of Observation. World Meteorological Organization, WMO-No.8.

WMO-No.544. (2003). Manual on Global Observing systems. World Meteorological Organisation- Annex V to the WMO Technical Regulations, Volume 1(No.544).

Appendix A: Results of Potential ET estimated from Penman Montieth Equation

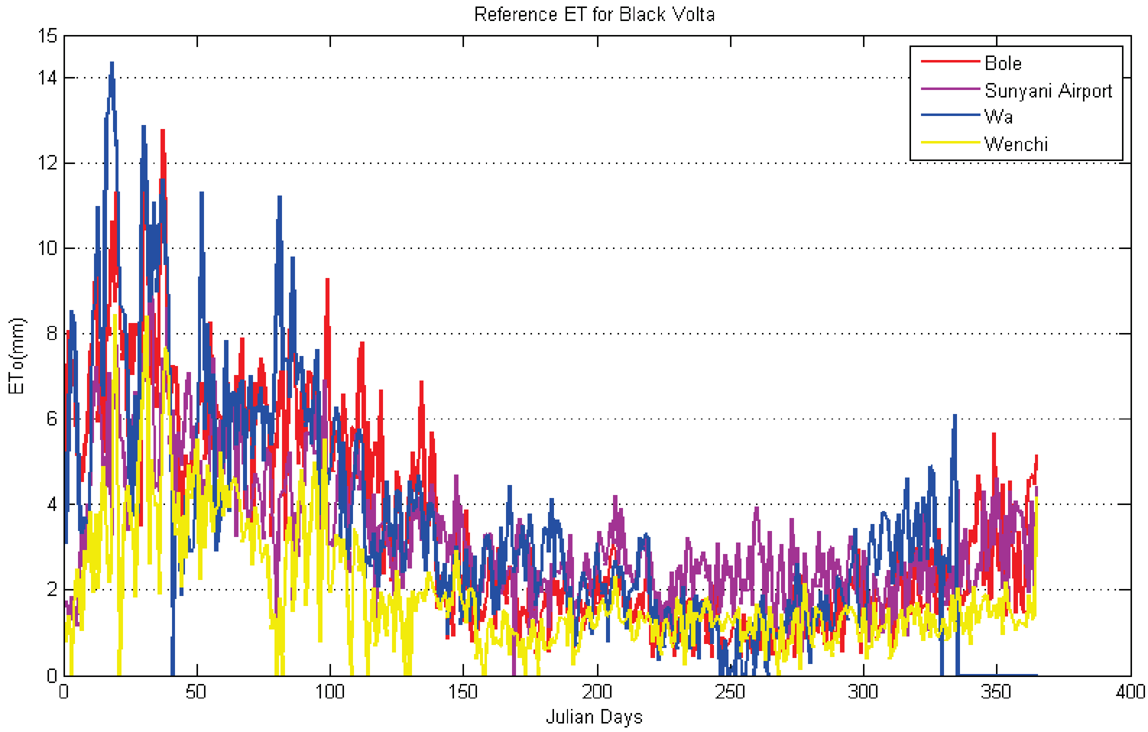

Figure 7:1 ET from Penman Montieth for Black Volta Basin

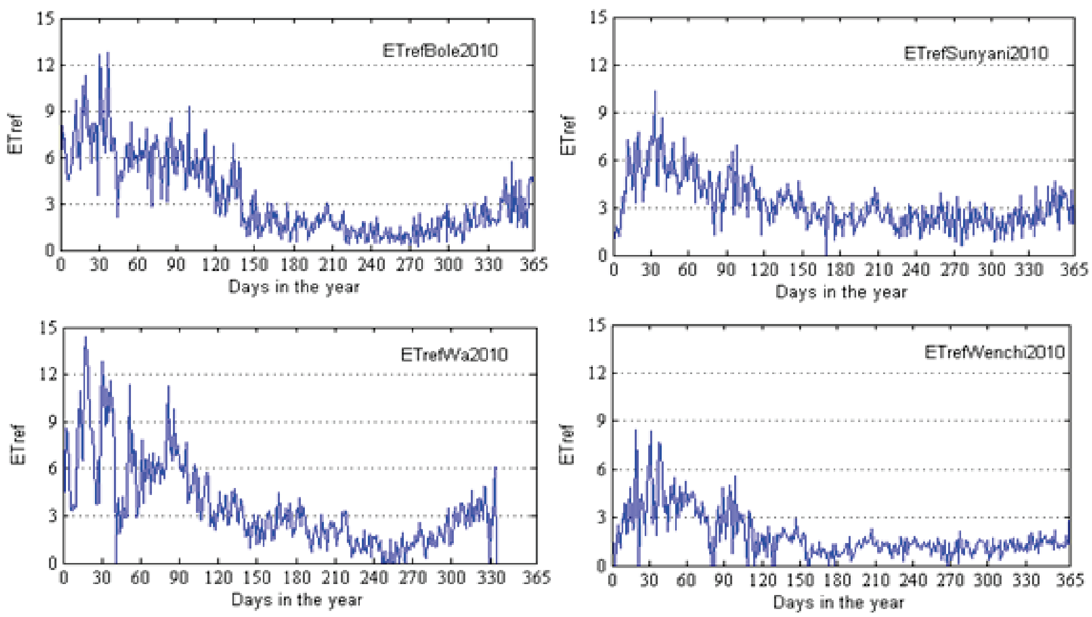

Figure 7:2 Individual Stations from Penman Montieth

Appendix B: Some Equations in SEBS ((Su, 2002),(Su, 2006).

Net Radiation

$$R_n = (1-\alpha)R_{swd} + \varepsilon_0 R_{lwd} - R_{out}$$

Shortwave Radiation

$$R_{swd} = I_{sc} e_0 \cos\theta \exp(-m\tau)$$

Longwave radiation

$$R_{lw} = \varepsilon\ \sigma T^{4}$$

The Obukhov Length

$$L = \frac{\rho C_p u_*^3 \theta_v}{kgH} \qquad \theta_v = \theta_a(1+0.61\mathrm{Q}) \qquad \theta_{0,a} = T_{0,a}\left(\frac{P_0}{P_{ref,s}}\right)^{0.286} \qquad \text{Eq.1}$$

$$u = \frac{u_*}{k}\left[\ln\left(\frac{z-d_0}{z_{0m}}\right) - \Psi_m\left(\frac{z-d_0}{L}\right) + \Psi_m\left(\frac{z_{om}}{L}\right)\right] \qquad \text{Eq.2}$$

$$\theta_0 - \theta_a = \frac{H}{ku_*\rho C_p}\left[\ln\left(\frac{z-d_0}{z_{0h}}\right) - \Psi_h\left(\frac{z-d_0}{L}\right) + \Psi_h\left(\frac{z_{oh}}{L}\right)\right] \qquad \text{Eq3}$$

Stability Functions

$$\Psi_m(y_s) = -\left[a_s y_s + b_s\left(y_s - \frac{c_s}{d_s}\right)\exp(-d_s y_s) + \frac{b_s c_s}{d_s}\right] \qquad \text{Eq.4}$$

$$\Psi_h(y_s) = -\left[\left(1 + \frac{2a_s}{3} y_s\right)^{1.3} + b_s\left(y_s - \frac{c_s}{d_s}\right)\exp(-d_s y_s) + \left(\frac{b_s c_s}{d_s} - 1\right)\right] \qquad \text{Eq.5}$$

Relative Evaporative Fraction

$$H_{wet} = \left((R_n - G) - \frac{\rho C_p}{r_{ew}}\frac{(e_{sat}-e)}{\gamma}\right)\Bigg/\left(1 + \frac{\Delta}{\gamma}\right)$$ Eq.6 ***Theoretical Wet limit***

$$r_{ew} = \frac{1}{ku_*}\left[\ln\left(\frac{z-d_0}{z_{0m}}\right) - \Psi_h\left(\frac{z-d_0}{L_w}\right) + \Psi_h\left(\frac{z_{om}}{L_w}\right)\right]$$ Eq.7 ***Resistance***

$$L_w = -\frac{\rho u_*^3}{kf0.61(R_n - G)/\lambda}$$ Eq.8 ***Wet – Obukhov length***

$$\Lambda_r = 1 - \frac{H - H_{wet}}{H_{dry} - H_{wet}}$$ Eq.9 ***Relative Evaporative Fraction***

kB-1

$$z_{oh} = \frac{z_{0m}}{\exp(kB^{-1})}$$ Eq.10

$$kB^{-1} = \frac{kC_d}{4C_t(u_*/u(h))(1 - e^{-n_{ec}/2})} f_c^2 + 2 f_c f_S \frac{k(u_*/u(h))(z_{0m}/h)}{C_t^*} + kB_s^{-1} f_s^2$$ Eq.11

$$n_{ec} = \frac{C_d LAI}{2(u_* / u(h))^2}$$ Eq.12

$$kB_s^{-1} = 2.46\left(\frac{h_s u_*}{\nu}\right)^{0.25} - \ln(7.4)$$ Eq.13

Appendix C: MODIS Technical Specifications

Orbit:	705 km, 10:30 a.m. descending node (Terra) or 1:30 p.m. ascending node (Aqua), sun-synchronous, near-polar, circular
Scan Rate:	20.3 rpm, cross track
Swath Dimensions:	2330 km (cross track) by 10 km (along track at nadir)
Telescope:	17.78 cm diam. off-axis, afocal (collimated), with intermediate field stop
Size:	1.0 x 1.6 x 1.0 m
Weight:	228.7 kg
Power:	162.5 W (single orbit average)
Data Rate:	10.6 Mbps (peak daytime); 6.1 Mbps (orbital average)
Quantization:	12 bits
Spatial Resolution:	250 m (bands 1-2) 500 m (bands 3-7) 1000 m (bands 8-36)
Design Life:	6 years

Appendix D: Standard error and Confidence Intervals

Date	Mean daily ETa(mm)	Standard error(mm)	Inter quartile range	Lower 95% Confidence limit(mm)	Upper 95% Confidence limit(mm)
1-Jan-10	5.64	0.01	0.13	5.61	5.66
3-Jan-10	3.92	0.04	0.49	3.84	4.00
5-Jan-10	3.83	0.08	0.66	3.68	3.99
6-Jan-10	5.17	0.02	0.32	5.12	5.21
7-Jan-10	5.12	0.02	0.19	5.09	5.16
8-Jan-10	4.18	0.08	0.43	4.02	4.33
9-Jan-10	5.25	0.05	0.28	5.16	5.35
10-Jan-10	2.96	0.06	0.81	2.84	3.07
12-Jan-10	3.02	0.05	0.67	2.92	3.12
13-Jan-10	5.79	0.08	0.13	5.62	5.95
14-Jan-10	4.63	0.03	0.36	4.57	4.68
15-Jan-10	5.08	0.06	0.31	4.97	5.19
16-Jan-10	4.70	0.02	0.30	4.66	4.75
17-Jan-10	3.45	0.05	0.71	3.34	3.55
18-Jan-10	5.79	0.06	0.13	5.67	5.90
19-Jan-10	5.25	0.02	0.37	5.21	5.30
21-Jan-10	5.06	0.03	0.43	5.00	5.11
22-Jan-10	5.55	0.02	0.26	5.51	5.59
23-Jan-10	5.79	0.02	0.29	5.75	5.82
24-Jan-10	5.09	0.04	0.45	5.02	5.16
25-Jan-10	5.87	0.01	0.15	5.85	5.89
26-Jan-10	5.30	0.02	0.27	5.26	5.34
29-Jan-10	5.63	0.14	0.34	5.36	5.90
30-Jan-10	4.05	0.04	0.50	3.98	4.12
31-Jan-10	3.85	0.05	0.69	3.76	3.95

Table 7:1Confidence Intervals for Bole.

Date	Mean daily ETa(mm)	Standard error(mm)	Inter quartile range	Lower 95% Confidence limit(mm)	Upper 95% Confidence limit(mm)
1-Jan-10	5.39	0.03	0.32	5.32	5.46
3-Jan-10	4.81	0.02	0.20	4.78	4.84
5-Jan-10	4.67	0.02	0.27	4.64	4.69
6-Jan-10	4.65	0.02	0.16	4.60	4.69
7-Jan-10	4.68	0.02	0.17	4.64	4.72
8-Jan-10	4.62	0.02	0.20	4.58	4.67
9-Jan-10	5.15	0.02	0.15	5.12	5.18
10-Jan-10	4.76	0.03	0.18	4.70	4.81
12-Jan-10	4.39	0.02	0.28	4.35	4.43
14-Jan-10	5.08	0.01	0.18	5.05	5.11
15-Jan-10	4.55	0.03	0.23	4.50	4.60
16-Jan-10	4.28	0.02	0.22	4.24	4.31
17-Jan-10	3.96	0.02	0.27	3.91	4.00
19-Jan-10	4.87	0.01	0.15	4.85	4.89
21-Jan-10	5.16	0.01	0.19	5.14	5.19
22-Jan-10	5.11	0.01	0.18	5.08	5.13
23-Jan-10	5.27	0.01	0.15	5.24	5.29
24-Jan-10	5.88	0.01	0.04	5.85	5.91
25-Jan-10	5.03	0.03	0.23	4.96	5.09
26-Jan-10	4.99	0.02	0.16	4.94	5.03
29-Jan-10	5.73	0.01	0.15	5.71	5.75
30-Jan-10	4.82	0.02	0.21	4.79	4.85
31-Jan-10	4.39	0.02	0.34	4.34	4.43

Table 7:2 Confidence Intervals for Wa

Date	Mean daily ETa(mm)	Standard error(mm)	Inter quartile range	Lower 95% Confidence limit(mm)	Upper 95% Confidence limit(mm)
3-Jan-10	5.28	0.044	0.89	5.19	5.37
12-Jan-10	5.99	0.015	0.20	5.96	6.02
17-Jan-10	6.01	0.033	0.18	5.95	6.08
21-Jan-10	5.21	0.131	1.21	4.96	5.47
28-Jan-10	5.44	0.056	0.11	5.33	5.55
30-Jan-10	5.99	0.016	0.20	5.95	6.02
31-Jan-10	6.37	0.004	0.04	6.36	6.38

Table 7:3 Confidence Intervals for Wenchi

Date	Mean daily ETa(mm)	Standard error(mm)	Inter quartile range	Lower 95% Confidence limit(mm)	Upper 95% Confidence limit(mm)
3-Jan-10	5.38	0.039	0.75	5.30	5.46
12-Jan-10	5.97	0.010	0.14	5.95	5.99
17-Jan-10	5.43	0.009	0.12	5.41	5.45
21-Jan-10	6.12	0.008	0.12	6.11	6.14
30-Jan-10	6.44	0.009	0.04	6.42	6.46
31-Jan-10	6.15	0.009	0.10	6.13	6.17

Table 7:4 Confidence Intervals for Sunyani

Appendix E: Histograms of errors in different stations

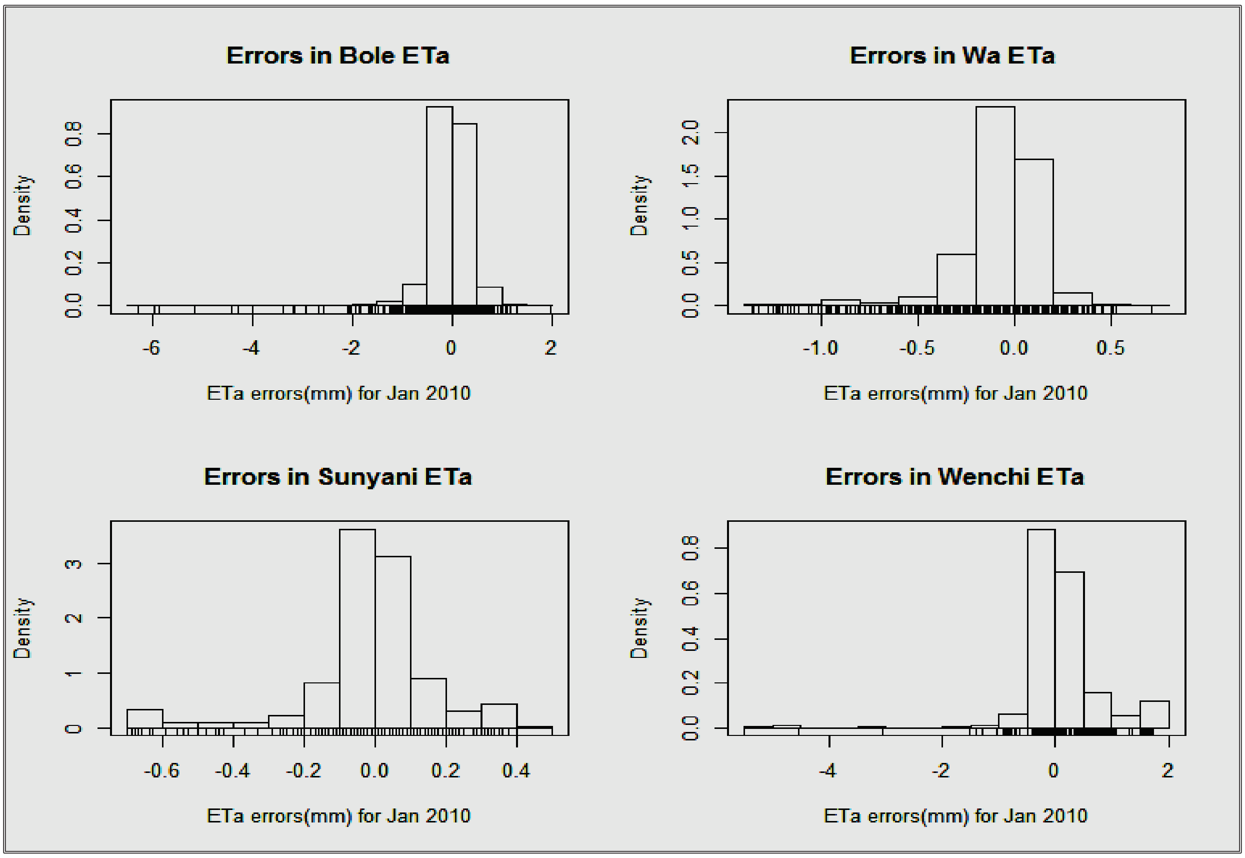

Figure 7:3 Errors in measurements. Baseline ETa and simulated

Mean Errors(mm) for Jan 2010							
Bole		**Wa**		**Wenchi**		**Sunyani**	
Date	**ME**	**Date**	**ME**	**Date**	**ME**	**Date**	**ME**
1-Jan-10	-0.03	**1-Jan-10**	-0.26	**3-Jan-10**	0.40	**3-Jan-10**	-0.08
3-Jan-10	0.02	**3-Jan-10**	-0.03	**12-Jan-10**	-0.02	**12-Jan-10**	0.01
5-Jan-10	-0.15	**5-Jan-10**	-0.02	**17-Jan-10**	-0.20	**17-Jan-10**	0.01
6-Jan-10	-0.02	**6-Jan-10**	-0.09	**21-Jan-10**	0.67	**21-Jan-10**	-0.01
7-Jan-10	-0.07	**7-Jan-10**	-0.13	**28-Jan-10**	-0.06	**30-Jan-10**	-0.02
8-Jan-10	-0.10	**8-Jan-10**	-0.12	**30-Jan-10**	-0.04	**31-Jan-10**	0.00
9-Jan-10	-0.09	**9-Jan-10**	-0.12	**31-Jan-10**	0.00		NA
10-Jan-10	0.08	**10-Jan-10**	-0.14		NA		NA
12-Jan-10	-0.01	**12-Jan-10**	0.00		NA		NA
13-Jan-10	-0.16	**14-Jan-10**	-0.02		NA		NA
14-Jan-10	-0.05	**15-Jan-10**	-0.08		NA		NA
15-Jan-10	-0.07	**16-Jan-10**	0.01		NA		NA
16-Jan-10	0.02	**17-Jan-10**	-0.01		NA		NA
17-Jan-10	-0.08	**19-Jan-10**	-0.04		NA		NA
18-Jan-10	-0.06	**21-Jan-10**	-0.01		NA		NA
19-Jan-10	0.02	**22-Jan-10**	0.00		NA		NA
21-Jan-10	0.01	**23-Jan-10**	-0.01		NA		NA
22-Jan-10	-0.02	**24-Jan-10**	-0.05		NA		NA
23-Jan-10	0.00	**25-Jan-10**	-0.21		NA		NA
24-Jan-10	-0.06	**26-Jan-10**	-0.10		NA		NA
25-Jan-10	0.00	**29-Jan-10**	-0.01		NA		NA
26-Jan-10	-0.01	**30-Jan-10**	-0.01		NA		NA
29-Jan-10	-0.64	**31-Jan-10**	-0.03		NA		NA
30-Jan-10	0.03		NA		NA		NA
31-Jan-10	-0.02		NA		NA		NA

Table 7:5 Mean Errors for ETa

RMSE(mm) for Jan 2010							
Bole		Wa		Wenchi		Sunyani	
Date	RMSE	Date	RMSE	Date	RMSE	Date	RMSE
1-Jan-10	0.13	1-Jan-10	0.43	3-Jan-10	0.59	3-Jan-10	0.40
3-Jan-10	0.40	3-Jan-10	0.16	12-Jan-10	0.15	12-Jan-10	0.10
5-Jan-10	0.80	5-Jan-10	0.15	17-Jan-10	0.39	17-Jan-10	0.09
6-Jan-10	0.22	6-Jan-10	0.24	21-Jan-10	1.47	21-Jan-10	0.08
7-Jan-10	0.18	7-Jan-10	0.24	28-Jan-10	0.56	30-Jan-10	0.09
8-Jan-10	0.80	8-Jan-10	0.27	30-Jan-10	0.17	31-Jan-10	0.09
9-Jan-10	0.48	9-Jan-10	0.21	31-Jan-10	0.04		NA
10-Jan-10	0.60	10-Jan-10	0.31		NA		NA
12-Jan-10	0.51	12-Jan-10	0.20		NA		NA
13-Jan-10	0.85	14-Jan-10	0.14		NA		NA
14-Jan-10	0.28	15-Jan-10	0.27		NA		NA
15-Jan-10	0.56	16-Jan-10	0.16		NA		NA
16-Jan-10	0.24	17-Jan-10	0.22		NA		NA
17-Jan-10	0.54	19-Jan-10	0.12		NA		NA
18-Jan-10	0.59	21-Jan-10	0.14		NA		NA
19-Jan-10	0.22	22-Jan-10	0.13		NA		NA
21-Jan-10	0.28	23-Jan-10	0.11		NA		NA
22-Jan-10	0.18	24-Jan-10	0.15		NA		NA
23-Jan-10	0.19	25-Jan-10	0.40		NA		NA
24-Jan-10	0.36	26-Jan-10	0.25		NA		NA
25-Jan-10	0.11	29-Jan-10	0.11		NA		NA
26-Jan-10	0.21	30-Jan-10	0.15		NA		NA
29-Jan-10	1.52	31-Jan-10	0.24		NA		NA
30-Jan-10	0.36		NA		NA		NA
31-Jan-10	0.48		NA		NA		NA

Table 7:6 RMSE estimates for ETa.

MONTE CARLO RUNS															
BOLE				WA				WENCHI				SUNYANI			
MeanETa (19runs)	SD	MeanETa (100runs)	SD	MeanETa (19runs)	SD	MeanETa (100runs)	SD	MeanETa (19runs)	SD	MeanETa (100runs)	SD	MeanETa (19runs)	SD	MeanETa (100runs)	SD
5.64	0.09	5.64	0.13	4.91	1.75	5.39	0.34	3.17	2.81	5.28	0.44	4.30	2.30	5.38	0.39
3.83	0.44	3.92	0.40	4.75	0.14	4.81	0.15	6.00	0.18	5.99	0.15	5.95	0.10	5.97	0.10
4.08	0.38	3.83	0.79	4.68	0.14	4.67	0.15	5.20	2.31	6.01	0.33	5.39	0.09	5.43	0.09
5.06	0.22	5.17	0.22	3.69	1.96	4.65	0.22	2.27	3.05	5.21	1.31	6.13	0.09	6.12	0.08
5.12	0.15	5.12	0.17	4.09	1.48	4.68	0.21	5.50	0.10	5.44	0.56	6.43	0.10	6.44	0.09
3.96	1.17	4.18	0.80	3.38	2.09	4.62	0.24	5.95	0.15	5.99	0.16	6.15	0.06	6.15	0.09
5.30	0.16	5.25	0.48	4.40	1.96	5.15	0.17	6.38	0.02	6.37	0.04				
2.90	0.63	2.96	0.60	4.51	1.11	4.76	0.27								
2.95	0.54	3.02	0.52	4.47	0.17	4.39	0.20								
5.59	1.35	5.79	0.84	5.09	0.13	5.08	0.14								
4.60	0.23	4.63	0.28	4.56	0.31	4.55	0.26								
4.92	1.20	5.08	0.56	4.31	0.17	4.28	0.17								
4.72	0.26	4.70	0.24	3.97	0.23	3.96	0.22								
3.51	0.51	3.45	0.53	4.89	0.11	4.87	0.12								
5.86	0.11	5.79	0.59	5.17	0.10	5.16	0.14								
5.29	0.19	5.25	0.22	5.07	0.14	5.11	0.13								
5.05	0.33	5.06	0.29	5.27	0.11	5.27	0.11								
5.60	0.18	5.55	0.18	5.57	1.36	5.88	0.14								
5.83	0.20	5.79	0.19	3.60	2.24	5.03	0.34								
5.16	0.29	5.09	0.36	4.96	0.28	4.99	0.23								
5.88	0.14	5.87	0.12	5.73	0.10	5.73	0.11								
5.39	0.22	5.30	0.22	4.74	0.18	4.82	0.15								
4.87	2.59	5.63	1.38	4.39	0.24	4.39	0.24								
3.96	0.41	4.05	0.36												
3.91	0.54	3.85	0.48												

Table 7:7 Comparisons on Monte Carlo Runs